

A Shared Metrological Framework for Trustworthy Virtual Experiments and Digital Twins

Original

A Shared Metrological Framework for Trustworthy Virtual Experiments and Digital Twins / Maculotti, Giacomo; Marschall, Manuel; Kok, Gertjan; Chekh, Brahim Ahmed; van Dijk, Marcel; Flores, Jon; Genta, Gianfranco; Puerto, Pablo; Galetto, Maurizio; Schmelter, Sonja. - In: METROLOGY. - ISSN 2673-8244. - 4:3(2024), pp. 337-363.
[10.3390/metrology4030021]

Availability:

This version is available at: 11583/2994181 since: 2024-11-06T10:59:09Z

Publisher:

MDPI

Published

DOI:10.3390/metrology4030021

Terms of use:

This article is made available under terms and conditions as specified in the corresponding bibliographic description in the repository

Publisher copyright

(Article begins on next page)

Article

A Shared Metrological Framework for Trustworthy Virtual Experiments and Digital Twins

Giacomo Maculotti ^{1,*}, Manuel Marschall ², Gertjan Kok ³, Brahim Ahmed Chekh ⁴, Marcel van Dijk ³, Jon Flores ⁴, Gianfranco Genta ¹, Pablo Puerto ⁵, Maurizio Galetto ¹ and Sonja Schmelter ²

¹ Department of Management and Production Engineering, Politecnico di Torino, Corso Duca degli Abruzzi 24, 10129 Turin, Italy; gianfranco.genta@polito.it (G.G.); maurizio.galetto@polito.it (M.G.)

² Physikalisch-Technische Bundesanstalt (PTB), Abbestraße 2-12, 10587 Berlin, Germany; manuel.marschall@ptb.de (M.M.); sonja.schmelter@ptb.de (S.S.)

³ Van Swinden Laboratory (VSL), Thijsseweg 11, 2629 JA Delft, The Netherlands; gkok@vsl.nl (G.K.); mvdijk@vsl.nl (M.v.D.)

⁴ Mechanical Engineering Unit, TEKNIKER, Calle I Goenaga 5, 20600 Eibar, Spain; brahim.ahmed@tekniker.es (B.A.C.); jon.flores@tekniker.es (J.F.)

⁵ IDEKO, Basque Research and Technology Alliance (BRTA), Arriaga Kalea 2E, 20870 Elgoibar, Spain; ppuerto@ideko.es

* Correspondence: giacomo.maculotti@polito.it

Abstract: Virtual experiments (VEs) and digital twins (DTs), pivotal for realizing European strategic policies on sustainability and digitalization within Industry 4.0 and the European Green Deal, simulate physical systems and characteristics in a virtual environment, with DTs incorporating dynamic inputs from and outputs to the real-world counterpart. To ensure confidence in their use and outcomes, traceability and methods to evaluate measurement uncertainty are needed, topics that are hardly covered by the literature so far. This paper provides a harmonized definition of VEs and DTs and introduces a framework for evaluating measurement uncertainty. Furthermore, it discusses how to propagate the uncertainty of the contributions coming from the different parts of the DT. For the core part of the DT, the framework derived for VEs can be used. For the physical-to-virtual (P2V) connection and the virtual-to-physical (V2P) connection, additional sources of uncertainty need to be considered. This paper provides a metrological framework for taking all these uncertainty contributions into account while describing a framework to establish traceability for DTs. Two case studies are presented to demonstrate the proposed methodology considering industrially relevant measuring instruments and devices, namely, a coordinate measuring machine (CMM) and a collaborative robot arm (cobot).

Keywords: virtual experiment (VE); digital twin (DT); measuring instrument; uncertainty; metrology; coordinate measuring machine (CMM); robot; collaborative robot arm (cobot)



Citation: Maculotti, G.; Marschall, M.; Kok, G.; Chekh, B.A.; van Dijk, M.; Flores, J.; Genta, G.; Puerto, P.; Galetto, M.; Schmelter, S. A Shared Metrological Framework for Trustworthy Virtual Experiments and Digital Twins. *Metrology* **2024**, *4*, 337–363. <https://doi.org/10.3390/metrology4030021>

Academic Editor: Han Haitjema

Received: 15 June 2024

Revised: 5 July 2024

Accepted: 14 July 2024

Published: 17 July 2024



Copyright: © 2024 by the authors. Licensee MDPI, Basel, Switzerland. This article is an open access article distributed under the terms and conditions of the Creative Commons Attribution (CC BY) license (<https://creativecommons.org/licenses/by/4.0/>).

1. Introduction

In the course of digitalization, the importance of modeling and simulating real-world processes in a computer is rapidly increasing. For example, nowadays, simulations are used to gain a better understanding of a corresponding real experiment or to support the planning of new experimental set-ups. In this development, the task of metrology institutes is to develop rules to ensure confidence in simulation results so that they can be used in a similar way as, or in conjunction with, real measurements.

In this paper, we distinguish between *virtual experiments* (VEs) and *digital twins* (DTs). Both are simulation models that accurately replicate physical systems and their characteristics in a virtual environment. In contrast with VEs, DTs also include dynamic updates of the virtual model according to the observed state of its real counterpart and a dynamic control of the latter. Hence, they include a *physical-to-virtual* (P2V) connection,

through which the physical entity is transferred into the virtual environment, and a *virtual-to-physical* (V2P) *connection*, which implements control strategies to achieve target results in the physical system [1].

In the literature, various definitions of the term “digital twin” can be found, covering a wide range of applications. The term “virtual experiment”, on the other hand, is almost exclusively used in the context of science education describing (interactive) simulations [2]. In other disciplines, the above-described simulation model without automatic data exchange between the physical system and the digital model (which will be called VE in this manuscript) is referred to as *virtual twin* [3], *computer model* [4,5], *digital model* [6], or simply *model* [7]. The following two paragraphs summarize the concepts of VEs and DTs as described in the literature.

1.1. VEs in the Literature

In ref. [8], a VE is stated to be *a numerical model of an experiment or a measurement process. It produces virtual data whose properties reflect those of the data observed in the corresponding real experiment.* A formal mathematical description of a VE using the notation of a statistical model with attention to the challenges in measurement processes is given in ref. [9]. In ref. [10], VEs are carried out to mimic the physical experiment and to investigate the behavior of the real measurement device. Illuminating the connection between a VE and the required digital representation of the measurement instrument, in refs. [11,12], the term *virtual instrument* is used for such a scenario. In this context, one of the main goals of the VE is to perform an uncertainty evaluation in conjunction with real measurement data, which will also be of primary interest in this work. In other publications where specific measurement devices and processes are modeled, similar terms describing their virtual representation are used, like *virtual coordinate measuring machine* (VCMM) in refs. [12,13], *virtual flow meter* in ref. [14,15], or *virtual tilted-wave interferometer* in ref. [10].

Another formal mathematical description of a similar concept can be found in refs. [4,5], where the term *computer model* is used for the implementation of complex mathematical models in computer codes.

In several publications, the concept that we call VE in this manuscript is only defined in the context of DTs, mainly with the aim of distinguishing the DT from general computing models and simulations [6]. In ref. [7], the term *model* is used. There, it is stated that *a DT without a physical twin is a model.* Chinesta et al. [3] use the term *virtual twin* for *emulating a physical system by one, or more, mathematical model to describe its complex behavior.* According to their definition, such *usual numerical models in engineering practice* are something static because they are not expected to be continuously fed by data so as to assimilate them [3]. In ref. [6], where the terms *digital model*, *digital shadow*, and DT are defined, the automatic flow of data is also the key aspect to distinguish between the three concepts. There, a digital model is *a digital version of a pre-existing or planned physical object [...] with no automatic data exchange between the physical model and digital model.* They state that *this means once the digital model is created, a change made to the physical object has no impact on the digital model either way.* A digital shadow, on the other hand, *has a one-way flow between the physical and digital object.* This means that *a change in the state of the physical object leads to a change in the digital object and not vice versa.* A flow of data in both directions then characterizes a DT. Here, *a change made to the physical object automatically leads to a change in the digital object and vice versa* [6].

1.2. DTs in the Literature

The concept of DTs was introduced by Grieves and Vickers from NASA as a *virtual representation of a physical object also containing digital information of such product* [16,17]. The DT concept was developed in the context of product life-cycle management, and has since been applied in many fields: predictive maintenance [18] and real-time control and monitoring of buildings and bridges for civil engineering [19], manufacturing technologies [20–22] and assembling [20,23] and disassembling [24] processes and related products [1], workflow for factory logistics [25,26], healthcare [27,28], energy applications for plants to optimize

resource production efficiency [29–31], and smart cities to control and optimize traffic and resources within an integrated IT framework [32,33]. Subsequent definitions tailored the concept, according to the needs of various application contexts in technological industries and fields distinguished by high automation capabilities, as those previously mentioned specifying, as depicted in Figure 1, that a DT includes the following:

- A *physical entity*, representing the entity the DT models and controls embedded in a *physical environment* tasked to carry out certain *physical process*; and
- A *virtual entity* fit in a *virtual environment*, i.e., the digital representation of the physical entity and its environment.

A further distinguishing element of a DT is the two-way *twinning*, i.e., the two-way automatic connection and data flow, between the physical and the virtual asset. In particular, it can be distinguished by a *P2V connection*, through which the physical entity is transferred to the virtual environment by means of sensors measuring relevant quantities to represent the current state of the entity, and a *V2P connection* aiming at controlling the physical entity and the physical process. The control is performed based on a decision-making engine embedded in the virtual environment. Specifically, the *virtual process* simulates and models the physical process based on the sensed and measured state of the physical entity and environment and predicts the next state of the system considering the task to carry out. Accordingly, based on the predicted outcome, control strategies can be deployed, by means of actuators through the V2P connection, to modify the state of the physical entity with the scope of optimizing the process and/or the outcome, i.e., preventing defects, out-of-control states, damages, etc. [1]. As a matter of fact, a DT cannot be considered as only data; rather, it shall include algorithms describing the asset's behavior and deciding on actions to deploy in the process [18,34], while predicting the system's response to unexpected events, before they occur, and preventing faults, damages, and hazards [18,35]. Measurement, and in particular metrology, covers a pivotal role in DTs since it ensures accurate measurement (i.e., sensing) and deployment (i.e., actuation) throughout the twinning phases [1].

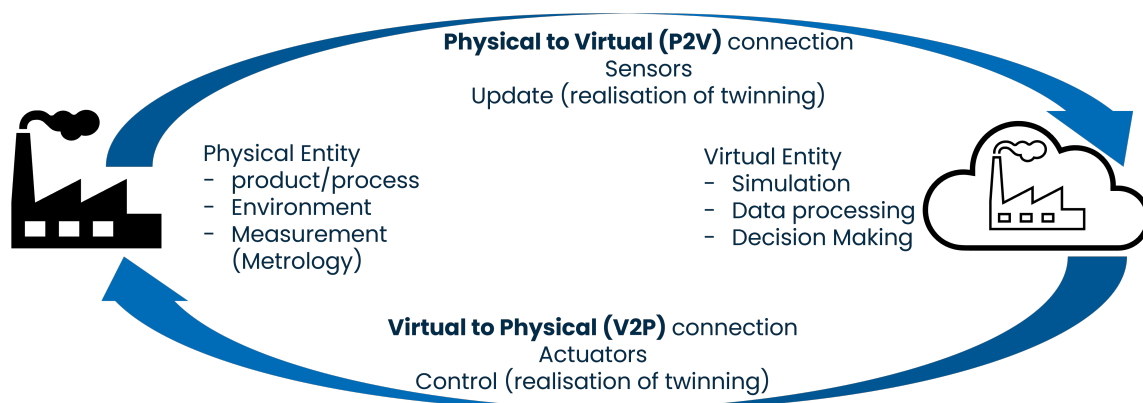


Figure 1. DT main components and scope.

Such a large adoption of DT technologies results in a massive literature, sometimes inorganic and providing manifold definitions for DTs [36]. Recent literature reviews [1,18,22,36,37] showed that, often, DTs are confounded with *digital models*, i.e., simulation or digital representations in which data flow manually from the physical to the virtual entity, thus being static, or with *digital shadows*, i.e., simulation models that are automatically updated to reflect the current state of the physical entity and environment, but with no automatic real-time control. The widespread interest in DTs has therefore led to the development of standards for the unambiguous definition of the concept.

Specifically, ISO 23247:2021 defines the DT as a *fit-for-purpose digital representation*, i.e., *data element representing a set of properties of an observable manufacturing element (OME), with synchronization between the element and its digital representation* [38]. ISO 23247:2021 specifies an Internet of Things framework to build and deploy DTs in manufacturing tech-

nologies. In particular, while highlighting the main features, e.g., fidelity and granularity (i.e., the representation detail of the DT), ISO 23247:2021, although not including it in the definition, specifies, according to the literature, the main applications, i.e., detection of anomalies, achievement of objective by real-time correction, off-line analytics, and predictive maintenance, while relying on the update rate, defined on a task-specific base, and relying on the previous and current state of the OME to analyze the current condition or predict its future state [38].

Similarly, ISO 30173:2023 defines the DT as *digital representation, i.e., a digital entity representing either a set of properties or behaviors or both of one or more observable elements of a target entity, i.e., an entity providing a functional purpose in reality, with data connections that enable convergence between the physical and digital states at an appropriate rate of synchronization* [39]. ISO 30173:2023 provides more general definitions of elements relevant and distinctive of the DT and its framework going beyond the manufacturing technology scope of ISO 23247:2021. Such generalization introduces the concept of a *DT system as a system providing functionalities for the DT composed of inter-operating target entities, digital entities, data connections, and models, data and interfaces involved in the data connection process*, and still includes, although not as a prominent feature, the *control loop* used to receive data from the target entity and issue back a signal to modify its behavior [39].

ISO standards particularly stress the difference between DTs and other typical enabling technologies of Industry 4.0. In particular, they point out that the two-way twinning and control loop is an essential feature of DTs, distinguishing them from VEs and other simulation models, and that Internet of Things is an enabling technology of DTs, which on its turn is an enabling technology for cyber-physical systems [39]. The twinning is realized by sensors (P2V) and actuators (V2P) whose metrology is of utmost relevance to establish traceability and guaranteed trustworthiness in the DT outcome. The standards [38,39] introduce some performance metrics and terminology, e.g., accuracy and fidelity, and state the relevance of performance verification and validation, which are consistent with the literature. However, the proper metrological assessment of performances, which caters to the concepts of traceability and measurement uncertainty, is not defined.

DTs are mostly applied to manufactured products during their mission operation [40] or to processes that are related to either manufacturing [41,42], logistics [26] or energy [29]. When considering complex systems, the DT can be viewed as a convolution in series and in parallel with many DTs exchanging information [43]. Thus, data exchange and the metrological traceability and trustworthiness of the data are of utmost relevance to associate confidence intervals with the outputs of the DT. Therefore, catering to uncertainty in the P2V twinning (i.e., sensing) and in the V2P twinning (i.e., of the actuators) is of utmost relevance to provide the confidence of usability of predictions, correction, and control workflow for quality management [35,44]. This becomes even more urgent when different systems are connected by DT technology or when the DT features and includes quality control processes [45–47].

The literature shows that, only since 2020 and the seminal paper of Karve et al. [48], the concept of measurement uncertainty has been introduced in DTs. Similarly, little attention has been paid to DTs of measuring instruments, and only recently, the role of metrology for digital twins (and vice versa) as been highlighted in [49]. Therefore, measurement uncertainty is becoming an urgent requirement for the holistic representation of manufacturing processes within cyber-physical systems using DT technology. The literature, to the best knowledge of the authors, reports only two applications, one tackling a fringe projection system [50] and another a coordinate measuring machine (CMM) [51,52]. In the latter one, also the concept of a *digital metrological twin (D-MT)* was introduced. Härtig et al. [52] define a D-MT as *a numerical model that depicts a specific measurement process and indicates an associated measurement uncertainty for a specific measured value, which is traceable to the units of the international system of units, having all parameters traceably determined and including traceable and validated measurement uncertainty*. The D-MT aims at describing a

complete measuring process and can be used in parallel with real measurements or for analyzing a real measurement (before or after the physical process).

1.3. Scope of the Work

The complex framework and incoherent literature of VEs and DTs have mostly focused either on developing enabling technologies (e.g., sensors, actuators, models, control algorithms) or, more recently, on implementing applications [1,18,22]. Conversely, awareness on the need to establish traceability and discuss the implications of measurement uncertainty on the different building elements has just recently risen [35,45,48,49,52]. The existing ISO 23247:2021 series establishes a framework and recommendations for implementing DTs in manufacturing. However, it does not encompass the aspects of verification, validation, and uncertainty quantification (VVUQ). The potential addition of a new section to ISO 23247:2021 focusing on this subject could offer guidance and methodologies for quantifying uncertainty, conducting DT testing, selecting or creating a credibility assessment framework for VVUQ activities, and evaluating the credibility of the developed DTs [53]. The European Union recently funded the international research project *trustworthy virtual experiments and digital twins* (ViDiT) [54] to advance metrological research on these topics and to fill the gaps mentioned above. To cope with that aim, and in response to the shortcomings highlighted in the literature, this work proposes a definition of VEs and DTs in such a way that these concepts are ready for use in metrological frameworks.

Specifically, this work presents a novel, formalized and harmonized definition of VEs and DTs for measuring and manufacturing equipment in technological industry applications as developed in the ViDiT project. Additionally, exploiting the proposed definition, a framework for the measurement uncertainty of VEs and DTs is proposed and discussed. In particular, the most relevant uncertainty influence factors, the requirements to establish traceability, and the main methodologies to evaluate measurement uncertainties are presented and discussed. Section 2 introduces the concepts of VEs and DTs mathematically and discusses them with respect to the reviewed literature. Section 3 discusses the main methods to evaluate the uncertainty of VEs and DTs, while highlighting the main challenges for traceability and uncertainty propagation. In Section 4, the uncertainty evaluation methods introduced above are applied to two test cases of industrial relevance, namely, a CMM (as an example for a VE) and an industrial robot (as an example for a DT). Lastly, Section 5 concludes on the findings and provides an outlook on future metrological research.

2. A Novel and Harmonized Definition of VEs and DTs

In the following, VEs and DTs are formally defined in such a way that they allow for uncertainty evaluation. Furthermore, the definitions are harmonized so that a VE can be seen as a core part of a corresponding DT. Hence, uncertainty evaluation methods for VEs can directly be applied to the corresponding part of a DT.

2.1. Definition of VEs

VEs are defined as mathematical/numerical models simulating, in a virtual environment, how the measurement data x , observed in a real experiment, are generated. To this end, the VE combines a deterministic mapping of certain input values with statistical elements that reflect the variability observed in a real experiment. Formally, we may write, following [9], a VE as a statistical model.

$$x = G(y, z, \epsilon), \quad \epsilon \sim F(E). \quad (1)$$

Here, y denotes a specific value for the measurand Y , which is the quantity of interest in a measurement and for which, ultimately, an uncertainty evaluation has to be performed. For example, in a CMM, Y denotes, e.g., the a priori unknown radius of a sphere that corresponds to the measurements of a spherical surface. The values z of the usually also multivariate parameter Z represent a variety of elements, e.g., parameters representing physical quantities, characteristics of the measurement instrument, variances

of error sources, and hyperparameters. In a real measurement, the actual parameter Z is unknown but fixed under repeated measurements. In contrast, ϵ , which is a realization of a random variable E with the distribution F , is a statistical parameter that varies in repeated measurements. These random influences additionally enter the mapping G , which reflects the real measurement process on a computer, and may influence the resulting virtual measurements x at any stage of the computation. Here, the mapping G might represent complex physical processes such as scatterometric principles in terms of the solution of partial differential equations, or it might model the effect of temperature deviations onto a measurement sensor.

While this general structure of a VE in (1) offers a much more flexible modeling approach, it also challenges the applicability of well-known approaches for uncertainty evaluation, such as the uncertainty evaluation framework of the *guide to the expression of uncertainty in measurements* (GUM) [55] or the Monte Carlo sampling approach defined in its supplements (JCGM 101 and JCGM 102) [56,57], which is due to the following difference.

The crucial difference to common uncertainty evaluation frameworks in metrology is that a VE takes values for the measurand as an input, whereas a measurement model [55], here also denoted by *data analysis* (DA), defines the (somewhat) inverse operation of the VE. In particular, the measurand quantity Y is the output of the DA, given the values for the measured (observed) quantity X and the model parameter Z . Since a measurement model is a mapping between quantities, one usually expresses the functional relationship by

$$Y = f(X, Z), \quad (2)$$

where f is sometimes called the “evaluation function” or “inverse model”. The latter is, however, misleading, since a measurement model in metrology might not be invertible. Moreover, given a VE as in (1), the choice of a measurement model is ambiguous, which has already been discussed for simple regression models in metrology [58], where the choice of the Euclidean norm for the optimization might not be sufficient for a corresponding measurement model. This is also discussed in ref. [59] for the CMM, where the impact of the choice of the measurement model is analyzed. In some cases, there might be no actual dependence on Z when applying the evaluation function to the quantity X , e.g., when fitting a sphere to measured coordinates. In other cases, there can be a dependence on Z ; e.g., in scatterometry, the wavelength of the light is needed to calculate the critical dimension of the sample from the measured light intensity [60]. Moreover, it is possible that the evaluation function depends on additional parameters that are not used in the VE but required for the DA, e.g., the degree of a polynomial that is fitted during the evaluation of the measurand [61].

In this work, we aim for a harmonized notation and definition of a VE and a DT to perform uncertainty evaluation for the measurand Y . While we define a VE in the general form (1) as a statistical model, which is to favor in a statistical setting, we employ in this work the simplified notation below to reduce the notation overhead when introducing the dynamics of a DT:

$$X = g(Y, Z). \quad (3)$$

With this notation, we absorb the statistical deviations and unknown but fixed parameter into the quantity Z and overall identify values and realizations with their quantity, denoted by uppercase letters. This means that X denotes the quantity corresponding to the measurements x , and the function g is therefore a mapping between quantities. Sometimes Equation (3) is referred to as observation equation [62].

Several approaches for uncertainty evaluation in the presence of a VE, a DA, and real measurement data have been proposed in the literature, notably [8,9] present approaches that are also in accordance with the GUM standards in metrology [56]. In this work, we will recall in Section 3.1 several uncertainty evaluation procedures for this purpose, and in Section 4.1, we demonstrate their feasibility for the VE of a CMM.

2.2. Definition of DTs

A DT is defined as a simulation model that accurately replicates a physical system in a virtual environment and that includes automated dynamic updates of the virtual model according to the observed state of its real counterpart to achieve an as-automated-as-possible physical control of the latter. The DT, according to the literature, consists of four parts:

- A physical environment, which embeds the physical entity(ies) to which the DT refers;
- A virtual environment with the virtual entities that models the considered physical asset(s);
- A P2V connection between the physical and virtual environments;
- A V2P connection that implements prevention and control strategies to achieve the target accuracy in the physical system, thus establishing a bi-directional data flow.

It is particularly interesting to notice the relationship with VEs, as defined in Section 2.1. Accordingly, a DT based on the data collected in the physical environment, fed to the virtual twin by the P2V twinning, estimates and predicts by the virtual asset of the state of the physical entity, and if needed, it deploys control strategies through the V2P connection. Then, if needed, the model can be updated to match the control; henceforth, the VE becomes time dependent, and as such, the virtual entity can be viewed as

$$X = g(Y, Z, t). \quad (4)$$

The time dependency underlays the re-calibration of the physical/virtual entity, update of the model domain (e.g., when considering self-learning machine learning approaches [63,64]), change of model due to modified control strategies, etc.

The DT definition introduced above is compliant with ISO 23247:2021 and ISO 30173:2023, while better clarifying the DT scope of control of the physical entity by means of the closed-loop feedback control and highlighting that a DT goes beyond a mere simulation and relies on automated data flow exchange, thus posing a clear distinction from the terms digital model and digital shadow. Furthermore, it is in line with the definition by Grieves [16,65], and it provides greater detail than the published ISO standards by stressing the three components of the DT, i.e., the physical entity, the virtual entity, and the twinning. In this context, it is relevant to point out that Grieves's concept of a DT, here adhered to by the definition in Section 2.2, is interpreted by ISO 30173:2023 as a *DT system*. Finally, as discussed previously, such definition finds a practical relevance in manufacturing technology and measurement fields, capable, at least in line with the principle, of great automation.

2.3. Connection between VEs and DTs

According to the previous discussion, both DTs and VEs involve a mathematical/software model of a certain physical entity, e.g., a measuring instrument. However, certain fundamental differences can be distinguished:

- A DT virtually mimics a real device by processing incoming sensor data in real time and can influence the real device by sending commands to its actuators, also in real time. A VE is conceptually something different. It simulates how measurement data are generated based on a simulated artifact and knowledge of the measurement instrument. However, the virtual entity of a DT can contain a VE, which is then modeling a measuring instrument, for example.
- A VE is especially useful when the relationship between a measurand and measured data is complex and/or indirect. The measurements performed for a DT might be straightforward to interpret by the DT model, or they may be indirect as well. The usefulness of a DT lies in the continuous monitoring and predictive maintenance and correction of physical systems, even when they are easy and simple to model.
- A DT shows the current state of several parts, as transmitted by auxiliary sensors, as well as the the result of the system's target operation, e.g., the measured quantity for a measuring instrument, the position for a machine tool, or process key performance indicators (KPIs) for a manufacturing system. In a VE, on the contrary, usually, only

the final measurement data are used. Therefore, the vector of measured data X is much longer for a DT.

- A DT must involve a dynamic, time-dependent, state-space model. A VE, on the other hand, assumes that the model does not change over time. It models either the current state of a measuring instrument (in case of a direct measurement) or the complete dataset that resulted from the entire measurement (in case of an indirect measurement). If the settings change, a new VE needs to be performed. Hence, a VE can be the “inner part” of a DT, which models the whole (time-dependent) process.

In summary, a VE can be used as sub-system of a DT. For example, it can be used to process (part of) the sensor data and estimate a measurand and its uncertainty, especially if there is a complex relationship. This measurement result can then be used by the DT model. A VE can also be used to estimate the main quantity of interest and its uncertainty. For example, a DT of a CMM gives the complete state of the machine in real time, whereas a VE is used to evaluate the complete dataset for a specific configuration, which does not change over time, and to calculate, e.g., the radius of a circle and its uncertainty based on all measured coordinates.

3. Uncertainty Evaluation for VEs and DTs

As mentioned in the introduction, establishing the traceability and evaluating the measurement uncertainty of VEs and DTs is essential to provide users with confidence in their exploitation. This section reviews the state-of-the-art methods to evaluate measurement uncertainty and to establish traceability for VEs and DTs. In particular, the main challenges will be highlighted, and approaches to overcome these will be proposed.

3.1. Uncertainty Evaluation Involving VEs

Uncertainty evaluation denotes the task of obtaining an estimate of the value of a measurand and its associated uncertainty, e.g., in terms of a standard uncertainty or a coverage interval, which describes the dispersion of the values being attributed to the measurand. The usual steps in metrological applications for uncertainty evaluation are the following: (1) Define a measurement model that relates all quantities involved in the measurement, and account for all systematic effects and instrument errors, e.g., in an explicit form as (2) or implicitly. (2) Values and uncertainties are assigned to relevant parameters and quantities. (3) A suitable propagation method for the uncertainties is chosen and applied, and the resulting estimate and associated uncertainty for the measurand are summarized. There are numerous possibilities to incorporate a VE into this process. The deterministic mapping of a VE that models the data generation process can be used as a forward model, and a Bayesian inference [66] for the measurand can be performed [61]. Assumptions on the forward model and a specific choice of the prior may ensure equivalence of a Bayesian inference to the JCGM 101 Monte Carlo approach, cf., e.g., ref. [67]. Additionally, refs. [8,9] perform uncertainty evaluation with equivalent results to the JCGM 101 uncertainty framework, using only the VE instead of a measurement model. Alternatively, the VE can be used to generate different measurement scenarios and analyze the effect of different parameters to assign realistic and relevant uncertainties [10]. In another approach, the data generation process of a VE can be used repeatedly in a Monte Carlo simulation study to enrich a small set of real measurements and analyze the resulting spread of the virtual measurements [68]. Finally, also the properties of uncertainty evaluation methods can be assessed using a VE. For a more in-depth overview of several methods for uncertainty evaluation, we refer, e.g., to ref. [59].

In this work, we focus on two example methods that apply either the *Law of Propagation of Uncertainty* (LPU) or the *Propagation of Distributions* (PoD) approach using Monte Carlo sampling. We will highlight for both approaches how a VE might be incorporated.

3.1.1. LPU-via-VE

“LPU-via-VE” stands for LPU evaluated using the VE. It assumes that the measurement model (or data analysis model) (2) is of the following form:

$$Y = f(X, Z) = \operatorname{argmin}_{Y'} \|X - g_0(Y', Z)\|_2^2, \tag{5}$$

where $X = g_0(Y, Z)$ denotes the VE without the addition of random measurement noise; i.e., the subscript $_0$ is used to indicate that a deterministic “forward model” is used instead of the model $X = g(Y, Z)$, which includes simulated random measurement noise. The estimate resulting from (5) is a (possibly local) optimum of the least-squares functional, and in this case, some algebraic manipulations based on the implicit function theorem can be performed to compute the associated uncertainty in terms of a covariance matrix ([57], clause 6.3).

$$U_Y = J_Y^{-1} J_{X,Z} U J_{X,Z}^T J_Y^{-T}. \tag{6}$$

Here, U_Y is the covariance matrix of the measurand Y , J_Y is the Jacobian of $-g_0(Y, Z)$ with respect to Y , and J_Z is the Jacobian of $-g_0(Y, Z)$ with respect to Z . The matrix $J_{X,Z}$ is a block-diagonal matrix containing the identity matrix of the same dimension as X and J_Z . If J_Y is rectangular, having more rows than columns but of full rank, J_Y^{-1} denotes the Moore–Penrose left-inverse matrix $(J_Y^T J_Y)^{-1} J_Y^T$ and J_Y^{-T} denotes its transpose. U denotes the covariance matrix of the vector (X, Z) , i.e., of both measurement data having the covariance matrix U_X and additional parameters Z having the covariance matrix U_Z . A schematic overview of this method is shown in Figure 2. It is also possible to split up the computation in separate terms addressing the uncertainty in X (“type A uncertainty”) and the uncertainty in Z (“type B uncertainty”) when X and Z are uncorrelated. This procedure is used in, e.g., ref. [69].

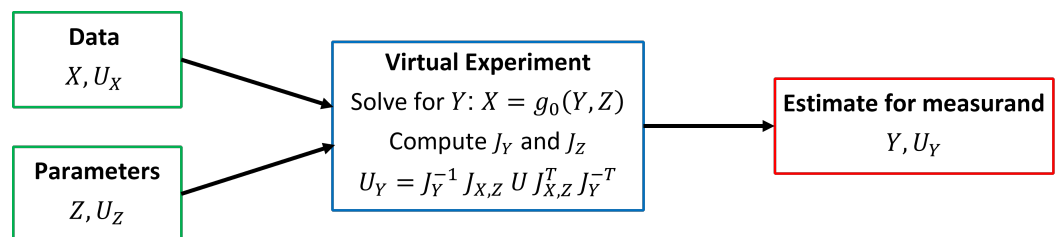


Figure 2. Schematic overview of the LPU-via-VE uncertainty evaluation method.

It is possible to extend this approach beyond the simple least-squares structure in (5) by accounting for the variability of the actual random parameter in the VE and adapting the functional appropriately. This might be realized by a maximum likelihood estimation or a Bayesian approach, which is, however, out of scope for this work.

3.1.2. PoD-via-VE

“PoD-via-VE” stands for PoD using the VE. The idea of this method is to use the VE to simulate how measurement data are affected by the error sources of the measurement process. This method can also be used to predict an uncertainty without any real measurements using purely simulated measurements. In Figure 3, a schematic overview of the method is shown for the case that real measurement data are available.

Based on the observed measurement data $x^{(\text{real})}$ and an estimate $z^{(\text{est})}$ of the parameter Z , an estimate $y^{(\text{sim})}$ of the measurand is calculated, together with some additional parameters relating to the artifact needed to run the VE. These parameters are then kept fixed. Then, the VE is repeatedly run using different random realizations $z^{(j)}$ of the uncertain parameter Z and of the measurement noise. This results in samples of simulated measurement data $x^{(j)}$. The data analysis function f can now be applied to $x^{(j)}$ and $z^{(\text{est})}$, resulting in samples $y^{(j)}$. From these samples, a distribution for the measurand can be derived, as

well as an estimate, a standard uncertainty, and a coverage interval. This procedure is used in, e.g., ref. [70].

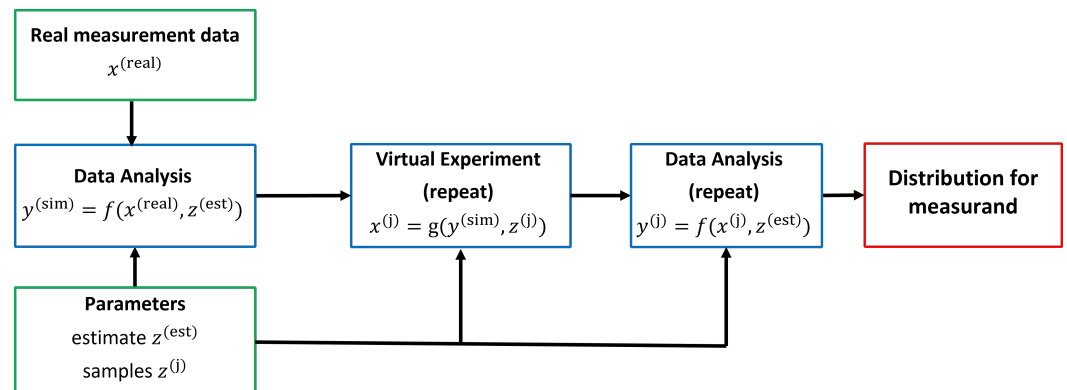


Figure 3. Schematic overview of the PoD-via-VE uncertainty evaluation method.

3.2. Uncertainty Evaluation for DTs

As far as measurement uncertainty and metrological characteristics of DT are concerned, only few papers, derived from the seminal work of Karve et al. [48], explicitly address and develop the issue of uncertainty evaluation in DT applications. Table 1 shows the main literature contributions, highlighting the distinctive features, incremental advancements provided by the work, and most relevant shortcomings. The literature distinguishes the uncertainty contributions as pertaining to the following three different categories:

- Uncertainty of the diagnosis, i.e., errors and uncertainties related to the sensors devoted to measuring the current state of the system;
- Uncertainty of the prognosis, i.e., errors and uncertainties related to the simulative model (e.g., VE) embedded in the virtual asset;
- Epistemic errors, i.e., errors to modeling strategy, which by extension include the fidelity and the twinning rate.

Such contributions are shared with uncertainty modeling for VEs, as discussed in the previous section. Additionally, for DTs, due to the automated bi-directional data flow, communication protocols quality and synchronization might induce further errors. The literature, in sparse additional cases [37,44], mentions the relevance of evaluating measurement uncertainty, but no quantitative examples are provided, and no methodology is reported. As shown in Table 1, the literature mostly resorts to Bayesian methods. In fact, although PoD [56] (abiding with conventional approaches [55]) or simulative methods are other viable approaches, dynamic Bayesian networks [48] and Bayesian statistics inherently allow automatic model updates to reflect the change of the state of the physical entity sensed by the sensors and/or induced by the actuators. However, how to include the stochastic nature of the control, thus catering to the feedback loop, in dynamic Bayesian networks, has not been discussed. The literature, indeed, remarks on the essential need to calibrate the diagnostic and prognostic model and states the need to propagate the uncertainty to cater to traceability. However, explicit methods used to propagate the uncertainty of several contribution and influence factors are not clearly reported, and some critical aspects are not explicitly remarked and discussed.

According to the literature, three main questions can be highlighted, as follows:

- How to establish traceability for a DT;
- How to define the uncertainty and accuracy of the P2V model;
- How to include the V2P correction and related uncertainty in the physical measurement of metrological characteristics and uncertainty.

Table 1. Literature review of papers discussing the evaluation of measurement uncertainty for DTs.

Authors and Year	Scope of the DT	Methodology for Uncertainty Evaluation	Limitations
Karve et al. [48]	Inspection planning for predictive maintenance and repair of fatigue loaded component	Bayesian approach to diagnose and predict (prognosis) defect formation to plan operation parameters	The method caters to systematic modeling errors and measurement uncertainty (even though not explicated). It does not discuss the issue of continuous update and closed-loop feedback control.
Nath and Mahadevan [71]	DT of a selective laser melting process	Dynamic Bayesian model to update the model prediction error, Gaussian process for the surrogate simulation model	The effect of the closed-loop control on the quality of the prediction is not discussed, nor uncertainty is evaluated.
Sisson et al. [72]	DT to predict stress in rotorcraft and plan mission	Bayesian approach for uncertainty and surrogate models to simplify physics modeling	The problem of the control looping on the uncertainty is not present because the control and prediction are not on the measured variable.
Ye et al. [73]	Reliability prediction	Data-driven approach based on a dynamic Bayesian network	Exteroceptive sensors to avoid update propagation of uncertainty due to the close-loop feedback control, but their uncertainty is not considered in the dynamic Bayesian network.
Thelen et al. [74]	Reviews the role of uncertainty and optimization of sensor placement	Detailed review of methods to estimate the uncertainty and methods to optimize the placements of sensors	The review highlights a lack of discussion in the literature on the correlation between the sensed state and the correction strategy (due to the iterative control) as well as the closed-loop feedback control correction typical of DT.
Huang et al. [75]	Introduces a framework for a holistic DT: innovatively mentions quality controls and measurements for DTs in the chain	Hybrid modeling and physics-informed machine learning	The contribution is essential, for it innovatively tries to include a D-MT in a DT of a larger process, but it provides a qualitative discussion and does not delve much on how to treat, estimate, and propagate measurement uncertainty.

This work attempts to reply to such questions and to motivate the need for the last point, i.e., the introduction of the uncertainty contribution due to the stochastic control, regardless of the method to estimate the uncertainty, e.g., Monte Carlo sampling [56] or Bayesian inference [48].

3.2.1. Problem Statement

According to definitions and notation introduced in Section 2, let us state and generalize the control problem associated with a DT. Let the physical asset (P) respond to a set of inputs W (environmental and external and internal describing the system state and thus controllable) to reach a target state Y measured by quantities X .

For example, let us consider a collaborative robot arm (cobot), whose Cartesian position in the working environment is the measurand Y , which is measured (X) by its angular encoders through Denavit–Hartenberg’s parameters, and depends also on the speed and type of the motion, these describing W . In the case of a measuring instrument, the instrument would respond to a certain measurand Y , under a set of measurement control variables and influence factors W , with a set of measurements X . For example, a surface topography measuring instrument will generate an electromagnetic surface X associated with a certain measurand surface Y , depending on measurement parameters W , e.g., light intensity, resolution, objective magnification, and the working principle.

Accordingly, the response X can be exploited to provide an estimate of the system state or of the measurand Y , i.e., \hat{Y} , by means of any DA function f . Thus, a P2V twinning can be established such that

$$X = g(Y, W, t; \theta), \tag{7a}$$

$$Y = f(X, Z, t) = f(X, W, t; \theta), \tag{7b}$$

where the parameters Z of Equation (4) are now expanded to include control and input parameters W and modeling parameters θ , which are the parameters of the mathematical function f .

Let us now assume that the physical system response is biased (Y_P), which can also be representative of a condition such that the physical system state Y_P is systematically different from the target Y aimed at by the control parameters W . In such a condition, the measured quantities X_P present a systematic error and, consequently, $f(X_P, W, t; \theta) = Y_P \neq Y$. Let this systematic error be E_X and E_Y , respectively, and suppose to have a calibrated external observer (C-EO) capable of estimating the measurement error E_X , and $f(X_{C-EO}, W, t; \theta) = Y_P$. Then,

$$E_X = X_P - X = X_{C-EO} - E_{X,C-EO} - X, \tag{8}$$

or, equivalently, the system state error E_Y

$$E_Y = Y_P - Y = Y_{C-EO} - E_{Y,C-EO} - Y. \tag{9}$$

For the sake of generality, the previous equations consider also the measurement errors of the calibration external observer $E_{\bullet,C-EO}$, where \bullet indicates any of the measurement X and the measurand Y . In general, the external observer should be calibrated and have $E_{\bullet,C-EO} \ll E_{\bullet}$, which could then be considered negligible.

For example, in the case of the robot arm depending on motion parameters W and even the position itself (i.e., the measurand Y), a systematic error in the positioning (e.g., a very high speed or a completely extended arm inducing poorer control) can be generated, which is typically measured only by a calibrated external observer. Similarly, in the case of a surface topography measuring instrument based on coherence scanning interferometry, a step height artifact Y will typically induce systematic errors at the step edges of the measured topography (X), the severity of which depends on the objective magnification (W) and the spacing of the steps (Y).

A DT is developed that aims at predicting E_{\bullet} and deploying some control strategies acting on controlling parameters W such that the error is minimized, leading to $Y_P = Y + o(Y) \sim Y$ and, consequently, $X_P = X + o(X) \sim X$. By calibrating a suitable model to estimate the systematic error E_{\bullet} , it is possible to correct the physical entity response. This is typically done by means of the DT loop involving the P2V connection, the prediction of the simulation (the virtual entity), and the control deployed in the V2P connection. To achieve that scope, the role of the calibrated external observer (C-EO) is pivotal. In fact, with $\{W, \theta\}$ leading to the system state $Y_P (\neq Y)$, it measures X_{C-EO} , estimating the actual system state Y_P , which allows achieving an unbiased response from the system as

$$X_{corr} = X_P - E_X = X_P - g_e(Y, W, t; \theta). \tag{10}$$

The correction term represented by g_e is the P2V twinning, representing a time-varying VE, which depends on the interaction of the system with the measurand Y , the environmental and control parameter W , and modeling parameters θ . Accordingly, it is worth noticing that the error is dependent on the input variables and also, in general, on the target response. The latter case is well exemplified by the position error of an industrial arm robot aiming to reach a certain position in the Cartesian working space. In such a case, the error depends on W , given by the payload, speed, type of motion, temperature, vibration, etc.,

but also on the target state Y , given by the position to be reached due to the non-infinite stiffness of joints and the arm length (the farther from the base in the horizontal direction, the larger the error).

It is relevant to remind that the internal observer in the system does not see the error it commits; thus, for the internal observer, the actual measurement and measurand are always equal to the target or the theoretical one. Thus, the role of the P2V twinning calibration by means of the calibrated external observer is again essential to allow a practical application of Equation (10), which can be rewritten as

$$X_{\text{corr}} = X_P - E_X = X_{\text{C-EO}} - g_e(Y_{\text{C-EO}}, W, t; \theta). \quad (11)$$

To achieve further generalization in this discussion, it is relevant to consider the application of DT to any given system, e.g., cobots. These are most typically controlled by motion parameters W . Therefore, the operation made explicit in Equation (11) aimed—ultimately—at implementing the condition

$$\begin{aligned} Y &= Y_P - E_Y = Y_P - (f(X_P, W, t; \theta) - f(X_{\text{corr}}, W, t; \theta)) \\ &= Y_P - (f(X_{\text{C-EO}}, W, t; \theta) - f(X_{\text{corr}}, W, t; \theta)). \end{aligned} \quad (12)$$

This entails controlling the system such that it targets $Y_P - E_Y$. Such condition can be obtained, indirectly, by combining Equations (11) and (12), or directly by finding a set of control parameters W^* capable of realizing such a condition. Here, it is worth remarking that how to make the system target $Y_P - E_Y$, i.e., how to find W^* , is problem dependent and task specific (for motion and position control of a robot, numerical or analytic approaches can be deployed, an inverse problem solution can be considered, etc.).

3.2.2. Establishing Traceability for a DT

Establishing traceability for a DT is a pivotal aspect to ensure the credibility, reliability, and accuracy of both virtual and physical systems in industrial applications. In the following, the key approaches to establish traceability in a DT environment are summarized.

Carmignato et al. [76] address the need for traceability by introducing dimensional artifacts as a link between the virtual and physical realms. These artifacts are essentially physical objects whose dimensions are known to have a high degree of accuracy, enabling them to serve as reference points for calibration in both digital and physical systems. For example, the assemblies with internally calibrated features are suggested to be used as dimensional artifacts in additive manufacturing processes. By focusing on the need for these artifacts to be calibrated to SI units and detailing how they should have well-defined measurands and uncertainties, the authors lay the groundwork for establishing traceability in advanced manufacturing environments involving DTs. Dahlem et al. [77] tackle the issue of traceability by introducing a holistic model for on-machine measurements. The novelty here lies in the model's capacity to use live process and environmental data to perform systematic error compensation and predict measurement uncertainty. This is achieved through a combination of novel spline-based models, data-driven thermal monitoring, and hybrid models that can adapt to both transient and static conditions. The paper is a comprehensive attempt to introduce traceability into live manufacturing settings. It even discusses future paths, like ISO standardization and the integration of machine learning, to make the system more robust and traceable. Jaganmohan et al. [78] turn their attention to optical measuring systems, particularly stereo vision systems. Using a standard test procedure (VDI/VDE 2634-1) as their foundation, they assess its sensitivity in detecting systematic errors. This is pivotal for establishing traceability as it offers a regulatory framework to adhere to. The authors simulate the effect of errors in camera parameters using a pinhole model, comparing these simulations with real-world measurements that were taken using a CMM as a benchmark. By proposing alternative, more sensitive, model-based lines, the study offers ways to improve performance evaluation and, by extension, traceability in DTs involving optical measurement systems.

In general, the traceability of a DT is established by the following:

- Calibrating the sensors with traceable material standards;
- Calibrating the model response by means of a comparison with traceable measurements with associated lower uncertainty and better accuracy; and
- Calibrating the actuators.

According to the discussion in Section 3.2.1, an essential step towards traceability is the availability of an external observer to enable the evaluation of the correction model $g_e(Y_{C-EO}, W, t; \theta)$. The calibration of such an external observer guarantees the traceability of the error correction.

3.2.3. Definition of Uncertainty and Accuracy of the P2V Model

The evaluation of the metrological characteristics of a DT is a concept poorly investigated in the literature. Metrological characteristics [79], like accuracy or precision, require an operative definition for the application to the DT framework, to cope with its time-dependent nature.

The literature reports several examples of evaluation methods for P2V twinning. Specifically, several methods have been made available and are discussed in the literature that resort either to Monte Carlo methods or to Bayesian approaches. The latter have gained quite a relevant role in allowing for a continuous update of the model, thanks to dynamic Bayesian networks. These networks also have the advantage to update the (prior) distribution of input-independent quantities on new observations that are taken at the twinning rate. For instance, Haitjema et al. [80,81] delve into the development of virtual measurements using calibration data from physical models. The Monte Carlo methods are used to simulate the effects of uncertainties in input quantities and to calculate the uncertainty of the measurand. Notably, they emphasized the need to preserve the autocorrelation function of deviations when simulating geometrical errors, such as scale and probe imperfections. In a similar vein, Ramu et al. [82] focus on the development of a virtual machine and a parametric model for a five-axis multi-sensor CMM. They incorporated calibrated artifacts and inverse kinematics to evaluate and correct geometric errors. Monte Carlo routines were applied for estimating task-specific uncertainties, thereby validating the effectiveness of their error correction algorithms. Dahlem et al. [77] propose an integrated framework that combines different modeling approaches to improve the accuracy and reliability of on-machine measurements. They introduced the concept of an abstracted physical body model to handle transient geometric errors under thermal loads. A data-driven framework for real-time thermal state prediction was also developed, emphasizing the need for a holistic approach that considers machine, workpiece, and environmental factors. In a more targeted approach, Vlaeyen et al. [83] showcase the development of a DT of an optical measurement system. The uncertainty was estimated by considering the error contributions from each component, such as the CMM, probe head, and laser line scanner. The model was validated using calibrated ring gauges. Lastly, Iñigo et al. [84] outline a methodology for simulating and analyzing the error mapping and compensation processes of a machine tool using a DT. Monte Carlo simulations were utilized to estimate the model's uncertainty, incorporating considerations like geometric errors and thermal variations.

In general, the P2V connection and the virtual entity represent sensing and simulation, i.e., a VE aiming at prognosis (i.e., predicting the system behavior) based on the diagnosis (i.e., the sensors). According to the literature, the model can be either analytical, data driven, or hybrid. Traceability—as discussed in Section 3.2.2—is established by calibrating the measurement instruments (i.e., sensors) required to gather the data for the model and by validating and testing the model. Evaluating the uncertainty of the model and of the P2V connection requires propagating the following four classes of contributions:

- The traceability of the sensors (coming from calibration certificates);
- The task-based influence factors to the measurement uncertainty of the sensors (i.e., the reproducibility, resolution);

- The model metrological performances (i.e., accuracy and precision); and
- Environmental conditions.

With a suitable experimental setup, involving proprioceptive sensors (i.e., internal sensors measuring x_p) and environmental sensors, it is possible to collect a set of data $\{x_p, w\}$; similarly, relying on proprioceptive, environmental, and exteroceptive (i.e., external) sensors, it is possible to collect $\{x_p, x_{C-EO}, w\}$. Note that we now use lowercase letters for realizations of the corresponding quantities, indicating actual measurements. Let \hat{X} be the output of the simulation model (or VE), i.e., the estimate, prediction, and prognostic of the virtual entity model g ; then an estimate of the actual state Y can be written as

$$\hat{Y} = f(x, w, t; \hat{\theta}) = f(g(y_{C-EO}, w, t; \hat{\theta}), z), \tag{13}$$

where w is the traceable system control input, $\hat{\theta}$ is the estimate of the VE model parameters, and z includes both system control inputs and some DA model parameters. Similarly, through the calibration external observer, the response error can be predicted and estimated as

$$\hat{E}_X = g_e(y_{C-EO}, w, t; \hat{\theta}), \tag{14}$$

where g_e is a function of the system state.

The model can be estimated by any statistic or machine learning approach that is mathematically and physically consistent with the problem at hand and with the constraint of the DT (e.g., model fidelity and modeling strategy). As usual, in statistics, the model parameters can be estimated by relying on collected data $\{x_p, x_{C-EO}, w\}$. The uncertainty of the simulation model (i.e., of the P2V connection and the virtual asset) can be evaluated by relying on methods to estimate measurement uncertainty of the modeling strategy. For an analytical model, this can be done by LPU; for data-driven approaches, simulative approaches as PoD [56] or non-parametric methods as Bootstrap [85] can be exploited.

The metrological characteristics of the P2V connection (i.e., focusing on accuracy and precision) can be evaluated by validating and testing the simulation model against a calibrated target, softgauge, etalon, higher precision measurement, etc. Precision can be evaluated by estimating the root mean square error of the model and by combining the variance of replicated measurements in reproducibility condition according to LPU.

At a certain time instant t , the accuracy of the physical system, as per the International Vocabulary of Metrology (VIM) [79], is defined as $Acc(Y, W, t; \theta) = g_e(Y, W, t; \theta)$. The DT aims at correcting any systematic error by means of the two-way interaction. Accordingly, data flow to the VE model in the P2V twinning to predict the expected error and correct it. Indeed, for the P2V twinning that is based on a stochastic model, a residual error $\epsilon \sim \mathcal{N}(0, \sigma_\epsilon^2)$ will result from the estimation of the model parameters θ and shall be considered in Equation (11). The calibration and evaluation of the accuracy of the P2V connection allows for establishing a traceable error mapping as a function of the considered input parameters of the DT. Accordingly, once the correction is deployed (at the time instant $t + \Delta t$ with $1/\Delta t$ being the twinning rate), the accuracy of the physical system is $Acc(Y, W, t + \Delta t; \theta) = \epsilon(Y, W, t; \theta)$. Nominally, the expected bias from the P2V twinning after the correction is $\mathbb{E}[Acc(Y, W, t + \Delta t; \theta)] = 0$.

Similarly, precision can be assessed in terms of reproducibility and repeatability. Once more, if the effect of error correction is considered, the P2V twinning expects a reproducibility of the physical entity after the implementation of the control of $\sqrt{Var[\epsilon(Y, W, t; \theta)]}$, i.e., the root mean square error of the residuals of the VE.

3.2.4. Effect of Closed-Loop Feedback Control on Measurement Uncertainty

Once the simulation embedded in the virtual entity predicted the response and the correction, the actuators should deploy the control strategy. Therefore, the metrological characteristics of the actuators introduce an additional source to the overall measurement uncertainty. Furthermore, the control loop and the presence of additional sensors (i.e., exteroceptive sensors) in the loop to enable real-time observation shall be catered

to. Another contribution to measurement uncertainty is given by sensor fusion, which is applied to monitor and predict redundancies in the system.

Overall, several influence factors, pertaining both to the physical and to the virtual entity, as well as to sensors, actuators, and the control strategies, shall be catered to, as depicted in Figure 4.

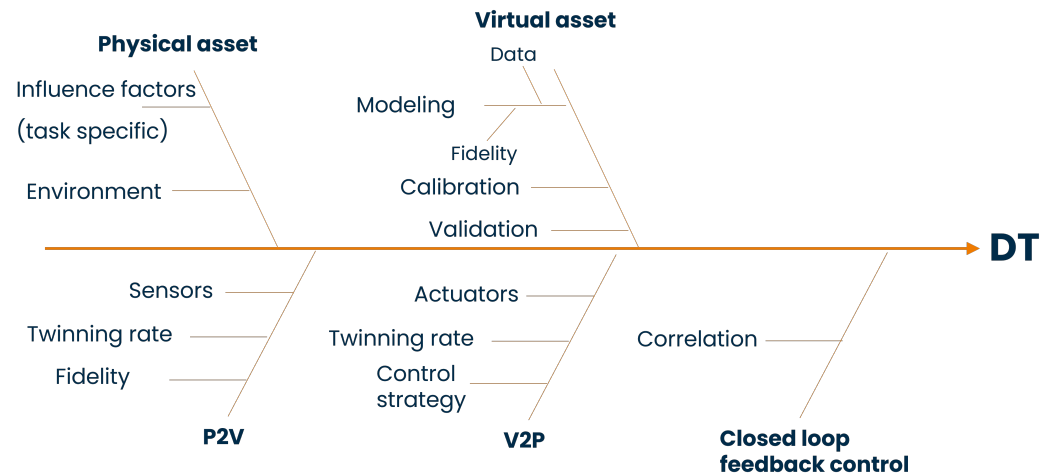


Figure 4. Main influence factors contributing to the uncertainty of DTs.

As highlighted in the literature review discussed in Section 1.2 and summarized in Table 1, the literature mostly resorts to Bayesian approaches to evaluate measurement uncertainty. Indeed, Bayesian statistics is inherently capable of managing time-dependent model updates. In particular, using the notation introduced in Equation (11), i.e., $\widehat{E}_X = g_e(y_{C-EO}, w, t; \widehat{\theta})$, once fixing the functional model of g_e and having a traceable external observer to gather y_{C-EO} and w , the problem is finding an estimate of the model parameters, $\widehat{\theta}$. Karve et al. [48] suggest resorting to Bayesian statistics so that, given prior assumption on the θ distribution, i.e., $p_{\text{prior}}(\theta)$, and an empirically determined likelihood $\mathcal{L}(y_{C-EO}|\theta)$, it results in the posterior

$$p_{\text{post}}(\theta|y_{C-EO}) \propto \mathcal{L}(y_{C-EO}|\theta) \cdot p_{\text{prior}}(\theta). \tag{15}$$

Indeed, there are also alternatives to Bayesian approaches; more traditional regression methods can also be exploited. However, since DTs perform iterative control of the physical entity and the model, in the most general case, they need continuous updates of the functional form and the model parameters [86]. The use of traditional approaches might lead to cumbersome updating methods, while Bayesian approaches inherently allow dynamic updates of model parameters. The knowledge of estimates of the model parameters θ and their distribution $p_{\text{post}}(\theta)$ is essential to enable uncertainty propagation of the expected measurement (or system state) of the physical entity after the control by the VE. The uncertainty evaluation can be done by following any applicable method, e.g., LPU [55,56], to Equation (11). This, according to Figure 4, shall then be combined with the uncertainty of the actuators.

Accordingly, once the control loop has been closed, the uncertainty of the measurement X_{corr} (or the system state Y) is a combination of the uncertainties of the control prediction (i.e., the time-dependent VE $g_e(Y, W, t; \theta)$ realizing the virtual entity), the actuators, and the sensing instruments (e.g., an external calibrated observer). Here, for the sake of simplicity, these uncertainties are propagated according to the LPU as follows:

$$u^2(X_{\text{corr}}) = u_{g_e}^2 + u_{\text{actuator}}^2 + u_{C-EO}^2, \tag{16}$$

where uncertainty contribution of the actuator and of the external observer sensors include both traceability and metrological characteristics, and the uncertainty due to the VE, i.e.,

$u_{g_e}^2$, depends on the functional model and, hence, includes contributions of the input data, $u^2(Y_{C-EO})$; control and environmental parameters, $u^2(W)$; and model parameters, $u^2(\theta)$.

3.3. Challenges

It is relevant to stress some shortcomings of the uncertainty evaluation approaches for DTs that can be found in the literature. First, when the system is in use, not always a calibrated external observer is exploited. This strongly challenges both model parameter estimation, as per Equation (15), and the uncertainty propagation, as per Equation (16). In fact, in both cases, the input data of the calibrated external observer y_{C-EO} would be replaced by data from an internal observer that are in generally biased (see Section 3.2.1) and more uncertain. This issue is currently not addressed in the relevant literature discussing uncertainty evaluation of DTs, although, in most applications, no sensor fusion of external observers is leveraged. Second, it is worth stressing that, under such conditions, the management and evaluation of measurement uncertainty catering to subsequent corrections of the physical system based on the stochastic model (the virtual entity, i.e., the VE embedded in the DT) are not discussed in the literature. Although the problem can be highly application specific, a general framework is still missing, which allows for coupling the sensor fusion with measurement uncertainty evaluation methods, e.g., LPU, Markov chain Monte Carlo, or Bayesian approaches.

4. Applications

In this section, the uncertainty evaluation methods introduced in Section 3 are applied to two test cases of industrial relevance. The first test case, which is an example for a VE, evaluates the uncertainty of a CMM by applying LPU-via-VE and PoD-via-VE. The second test case, which is an example for a DT, applies the uncertainty evaluation methods introduced in Section 3.2 to a cobot.

4.1. VE of a CMM

In this section, we present an example of a metrological application in which the uncertainty of the measurand is evaluated using a VE of the form (3). The general ideas of the uncertainty evaluation methods presented in Section 3.1 will be adapted such that the methods can be applied in the CMM context.

4.1.1. Description of the Application

The application of interest is the evaluation of the radius R and roundness P_v of an approximately circular shape based on a set of n measured two-dimensional point coordinates $(x_{1,i}, x_{2,i})$, $1 \leq i \leq n$, measured by means of a CMM. These coordinate data together constitute the observed value of the measured quantity X in Equations (2) and (3). The roundness is quantified by the so-called peak-to-valley value, in short, pv-value, P_v , which equals the maximum distance from the rim of the fitted circle (peak) minus the minimum (signed) distance (valley) from the circle rim of the measured points [87]. This quantity is also equal to the difference of the maximum and minimum point distances to the fitted circle center.

The VE of the CMM models how the measured coordinates are generated based on an assumed shape of the artifact being measured. In such a simulation, many more parameter values are needed than just the assumed values for the measurand. In this case, the following parameters are required:

$$\mathbf{y}_{ve} = (r, c_1, c_2, \phi_1, \dots, \phi_n, n_{lobes}, \phi_{lobes}, a_{lobes})^T. \quad (17)$$

Here, r denotes the circle radius, (c_1, c_2) are the coordinates of the circle center, and the angles ϕ_1 to ϕ_n denote the angular position of the measured points on the circle. To simulate

an imperfect circle, n_{lobes} lobes were included by adding a sine-wave-based perturbation to the radius. This means that the distance of the point i to the circle center is given by

$$r_i = r + a_{lobes} \sin(n_{lobes}\phi_i + \phi_{lobes}), \tag{18}$$

where a_{lobes} denotes the amplitude of the lobes and ϕ_{lobes} denotes an offset angle. The simulated artifact shape by the VE should be sufficiently close to the shape of the real artifact, though this correspondence might not be exact. Note that there is no value corresponding to the second component P_v of the measurand included in y_{ve} , although it holds that $P_v = 2a_{lobes}$ in this simple model. The true simulated artifact coordinates $(x_{art,i}, y_{art,i})$ are given by

$$\begin{pmatrix} x_{art,i} \\ y_{art,i} \end{pmatrix} = \begin{pmatrix} c_1 \\ c_2 \end{pmatrix} + r_i \begin{pmatrix} \cos \phi_i \\ \sin \phi_i \end{pmatrix}. \tag{19}$$

The additional parameters of the VE corresponding to the quantity Z in (1) are given by

$$\mathbf{z}_{ve} = (s_x, s_y, s_{xy}, \sigma)^T. \tag{20}$$

Here, s_x denotes a linear scale error of the x -axis of the CMM, s_y denotes a linear scale error of the y -axis, s_{xy} models the squareness error between x - and y -axis [88], and σ denotes the standard deviation of the measurement noise. The first three error sources can be combined in a matrix.

$$A = \begin{pmatrix} 1 + s_x & 0 \\ (1 + s_x)s_{xy} & 1 + s_y \end{pmatrix}. \tag{21}$$

Besides these systematic errors, the measured coordinates of point i are affected by measurement noise $\epsilon_{1,i}$ and $\epsilon_{2,i}$, which are independent and identically distributed with a Gaussian distribution with mean zero and standard deviation σ . The relationship between true coordinates $\mathbf{x}_{true,i}$ of point i , expressed in a Cartesian reference coordinate system, and its measured coordinates $\mathbf{x}_{meas,i}$, as returned by the CMM, is given by

$$\mathbf{x}_{meas,i} = A\mathbf{x}_{true,i} + \begin{pmatrix} \epsilon_{1,i} \\ \epsilon_{2,i} \end{pmatrix}. \tag{22}$$

By combining the equations of this section, the VE function g and its noise-free version g_0 can be deduced. For specific values of the variables, this then leads to $\mathbf{x}_{meas} = g(\mathbf{y}_{ve}, \mathbf{z}_{ve})$. An example of a simulated lobed circle with a relatively large lobe amplitude a_{lobes} for better visibility is shown in Figure 5.

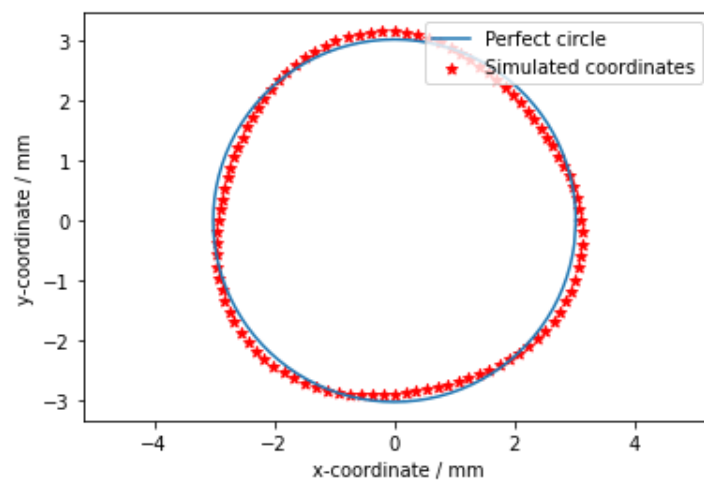


Figure 5. Example of simulated lobed circle by means of the VE.

In the next two sections, we will discuss how this VE can be used to evaluate the measurement uncertainty using two different methods.

4.1.2. LPU-via-VE

To use LPU-via-VE, first, an estimate $\hat{\mathbf{z}}_{ve}$ is required, which we set to $(0, 0, 0)^T$ in this example. Then by a least-squares circle fit routine applied to the measured data \mathbf{x} , estimates of r , c_1 , and c_2 can be determined. Using these estimates and the data, also estimates of ϕ_1, \dots, ϕ_n , n_{lobes} , ϕ_{lobes} , and a_{lobes} can be obtained, which solve Equation (5) in good approximation and result in a $\hat{\mathbf{y}}_{ve}$. Using $\hat{\mathbf{y}}_{ve}$, $\hat{\mathbf{z}}_{ve}$, and the derivatives of g_0 , the (relevant part of the) covariance matrix U_Y can be computed following Equation (6). From this computation follows the standard uncertainty $u(\hat{r})$ of the radius estimate \hat{r} . An estimate \hat{p}_v of the value of P_v is obtained from the difference of the maximum and minimum point distances to the fitted circle center, i.e., $\hat{p}_v = \max_{1 \leq i \leq n} \hat{r}_i - \min_{1 \leq i \leq n} \hat{r}_i$ with the distances \hat{r}_i calculated based on the estimated circle center, i.e., $\hat{r}_i = \|x_i - (\hat{c}_1, \hat{c}_2)^T\|$. This is preferred over the alternative of deriving an estimate from the fitted shape given by $\hat{\mathbf{y}}_{ve}$ directly in order to allow for a real shape that somewhat deviates from a sine-based-lobed shape. The standard uncertainty $u(\hat{p}_v)$ follows from applying the LPU, whereby the calculated uncertainties of the center coordinates are used.

4.1.3. PoD-via-VE

We now describe the implementation of the method PoD-via-VE for the CMM application. As a first step, an estimate $\hat{\mathbf{y}}_{ve}$ of the VE parameters is determined in the same way as for LPU-via-VE in the preceding section. This fixes the artifact shape that is being used in the VE. As a next step, a Monte Carlo method is applied, in which samples $\mathbf{z}^{(j)}$ are drawn for the VE parameters based on the provided distributions, as well as samples $\epsilon_{1,i}^{(j)}$ and $\epsilon_{2,i}^{(j)}$ modeling the measurement noise for each of the points i with $1 \leq i \leq n$, based on the provided σ . Using the VE, samples of simulated measurement data $\mathbf{x}^{(j)}$ can now be calculated. By applying the circle fit routine to each simulated dataset, samples $r^{(j)}$ and $p_v^{(j)}$ of the radius and pv-values are obtained, from which a statement of the uncertainty can be obtained.

4.1.4. Numerical Results

We performed a numerical experiment using the VE for the CMM as described in Section 4.1.1 and applied the LPU-via-VE and PoD-via-VE methods. For this purpose, measurement data were simulated with parameter values as listed in Table 2.

Table 2. Parameter values used for generating simulated measurement data.

Parameter	n	r / mm	c ₁ / mm	c ₂ / mm	n _{lobes}	φ _{lobes} / rad
Value	1000	3.01764	0.00100	0.00245	3	1
Parameter	a _{lobes} / mm	s _x	s _y	s _{xy} / rad	σ / mm	
Value	0.05000	0.00005	0.00011	0.00020	0.00050	

The standard uncertainties of the error sources (input quantities) that were used in the uncertainty evaluation are shown in Table 3.

Table 3. Standard uncertainties of the error sources used for the uncertainty evaluation.

Parameter	u(s _x) / rad	u(s _y) / rad	u(s _{xy}) / rad	σ / mm
Value	0.00012	0.00012	0.00012	0.00050

In Table 4, the calculated estimates and standard uncertainties according to the two methods are shown for a single simulation. In the PoD-via-VE method, 100,000 samples

were used when applying the Monte Carlo method. For the radius, the results are identical. For the pv-value, the results differ somewhat, which is due to the fact that the calculated pv-value typically increases in the presence of CMM errors. The employed DA for evaluating the pv-value is thus somewhat biased when comparing it with the ground truth value of the simulation. This effect is more pronounced in the PoD-via-VE method. In Figure 6, the calculated distributions for the radius and pv-value are shown for the two employed methods. The distributions are virtually identical for the radius, but not for the pv-value. In the case of LPU-via-VE, a Gaussian distribution with the calculated mean and standard deviation is used.

Table 4. Estimates and standard uncertainties for the radius and pv-value for the LPU-via-VE and PoD-via-VE methods.

Method	\hat{r} / mm	$u(\hat{r})$ / mm	\hat{p}_v / mm	$u(\hat{p}_v)$ / mm
LPU-via-VE	3.01787	0.00025	0.10022	0.00032
PoD-via-VE	3.01787	0.00025	0.10045	0.00027

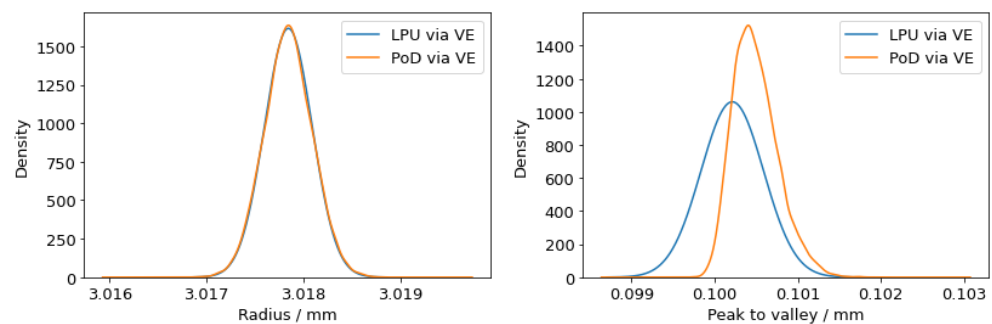


Figure 6. Distributions for the radius (left) and pv-value (right) calculated according to two different uncertainty evaluation methods involving the VE.

4.2. DT of a Cobot

In this section, we present an application of a metrological and traceable DT for a cobot. The case study is demonstrated on an industrial cobot, Yaskawa MOTOMAN HC20DTP, with a maximum payload of 20 kg equipped with a gripper. The task that the DT aims at monitoring and controlling is the accurate and precise positioning of the end effector, i.e., the gripper, while holding a weight of 5 kg. An accurate and repeatable positioning of components is essential to allow efficient and effective collaboration in a manufacturing environment to improve ergonomics and avoid assembling errors [24,89,90]. A typical acceptable positioning error is within ± 0.5 mm.

The measurement of the position of the end effector can be performed by relying on internal angular encoders, which, although calibrated at the factory level, could present bias. In this work, a DT is developed to improve the position accuracy and correct systematic errors. In particular, an external set of eight cameras, namely, OptiTrack PrimeX 22, working on infrared wavelength and capable by a proprietary machine vision algorithm of recognizing passive retro-reflectors, is exploited to monitor in real time the actual position of the cobot end effector. The machine vision system (MVS) has a resolution of 5 μ m in the working volume and was calibrated with a laser tracker showing a measurement uncertainty of 0.150 mm, i.e., $u_{C-EO} = 0.075$ mm. Figure 7 shows the experimental setup at the MInd4Lab at Politecnico di Torino.



Figure 7. Yaskawa cobot and OptiTrack cameras (black cubes with a blue ring in the picture) used for the DT case study.

Typically, the positioning of the cobot is intuitively and indirectly programmed by indicating the end position of the Tool Center Point (TCP) as a set of Cartesian coordinates $TCP = (TCP_x, TCP_y, TCP_z)$ with respect to the base of the cobot. Here, it is worth remarking that the system state, i.e., the measurand, is the position of the TCP, which can be measured in terms of its Cartesian coordinates (TCP_x, TCP_y, TCP_z) . The positioning accuracy can be expressed as the error of the actual position TCP_{eff} with respect to the nominal position TCP_{nom} . This error can, in terms of Cartesian distance, be written as

$$d_e = \|TCP_{eff} - TCP_{nom}\|_2 \quad (23)$$

$$= \sqrt{(TCP_{x_{eff}} - TCP_{x_{nom}})^2 + (TCP_{y_{eff}} - TCP_{y_{nom}})^2 + (TCP_{z_{eff}} - TCP_{z_{nom}})^2} \quad (24)$$

Accordingly, the actual position for the internal encoders, i.e., TCP_{int} , is always equal to the nominal position TCP_{nom} such that $d_e = \|TCP_{int} - TCP_{nom}\|_2 = d_{int} - d_{nom} = 0$, where d_{int} and d_{nom} indicate the distance of the corresponding TCP from the origin of the relevant coordinate reference system. Thanks to external sensors, the position error, on the other hand, can be evaluated in this case by the MVS such that $d_e = \|TCP_{eff} - TCP_{nom}\|_2 = \|TCP_{MVS} - TCP_{nom}\|_2$. The P2V twinning is established by evaluating the positioning error as a function $g_e(Y, W, t; \theta)$, where the measurand Y is the actual position of the TCP, which can be measured (X) as its Cartesian coordinates, and system parameters W are influence factors and motion control parameters, e.g., the type of motion and the motion speed. Model parameters θ have to be estimated by appropriate statistical modeling. In this work, a Gaussian process regression (GPR) is used to model g_e . To train the model, 21 points were considered in the motion volume of the cobot. Positions were measured with internal angular encoders and the MVS, thus enabling the evaluation of the accuracy. To cater to the reproducibility of the actuators, nine replications were performed. The 21×9 randomly spaced points were then replicated three times considering, according to the literature [89], as most relevant factors the motion speed on three levels $v = [20\%, 60\%, 90\%]V_{max}$, and only considering the linear joint motion. In this work, a simplified condition that does not consider the effect of different payloads is considered.

The MVS camera system allows for identifying the positioning distance error of the system as is. Figure 8 shows the initial conditions (red circles), which present an average error $\overline{d_e}$ of 2.012 mm and a standard deviation $s(d_e)$ of 0.256 mm.

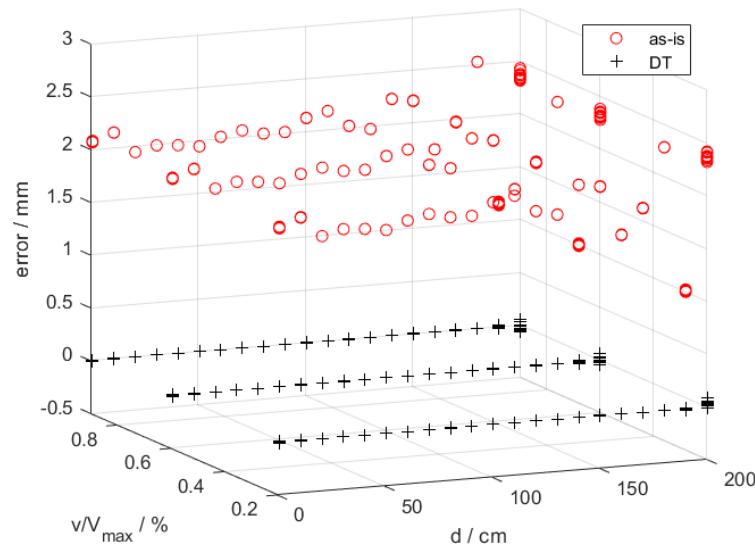


Figure 8. TCP positioning error of the cobot as is (red circles) and after the implementation of the DT (black crosses).

The P2V model results in estimating the $g_e(Y_{C-EO}, W, t; \theta) = g_e(TCP_{eff}, v, t; \theta)$. In this case study, considering the spatial correlation of the errors due to the finite compliance of the system, which is also increasing with the distance d of the TCP from the base, a GPR model was selected. In particular, the GPR modeling the error was a function of the system state Y represented by the TCP position, the control parameters W being the motion speed v and model parameters $\theta = (\beta, \sigma_y^2, \sigma_l^2)^T$, consistent with a linear basis function with an estimated matrix $\beta = [2, 1.897, 0.164]$ and a squared exponential kernel $\mathbf{R} = \sigma_y^2 \exp(-\frac{1}{2} \frac{(h_{ij}^T h_{ij})}{\sigma_l^2})$ modeling the covariance with $h_{ij} = ((d_i, v_i) - (d_j, v_j))^T$ and estimated variance of the process $\sigma_y^2 = 1.374 \text{ mm}^2$ and a location scale parameter $\sigma_l = 24.89 \text{ mm}$. In this case study, the parameters θ_R of the GPR and the specific basis and kernel function were optimized by a Bayesian procedure to test multiple alternatives by means of an operator-agnostic way [86]. The residuals of the model $d_{e,res}$ presented a mean $\overline{d_{e,res}} = \widehat{d_e} - d_e$ of $0.4 \text{ }\mu\text{m}$ and a standard deviation $s(d_{e,res})$ of $9.3 \text{ }\mu\text{m}$.

The P2V twinning allows for correcting the position of the cobot. In fact, given a certain nominal destination d_{nom} and motion speed v , the P2V GPR predicts the positioning error $\widehat{d_e} = g_e(d, v, \theta)$. Figure 8 shows the residual errors after the implementation of the V2P twinning, realizing the DT control.

Measurement uncertainty is then estimated to assess the statistical relevance of the control withing a metrological framework. In this case study, a GUM-LPU approach is applied, consistent with Equation (16). In particular, it is interesting to notice that the uncertainty contributions of the actuators $u_{actuator}^2$ are estimated inherently by means of the implemented experiment, and henceforth, they are implicitly included in the variance of the measured positioning error. Furthermore, to assess the effectiveness of the implemented

DT, the uncertainty of the positioning can be evaluated for the system as is and after the DT application in a new $\{d^*, v^*\}$, thus being

$$u(d) = \sqrt{u_{acc}^2 + u_{trac}^2 + u_{reprod}^2}, \tag{25a}$$

$$u(d_{as-is}(d^*, v^*)) = \sqrt{\frac{d_e^2}{3} + u_{C-EO}^2 + s^2(d_e)}, \tag{25b}$$

$$u(d_{corr}(d^*, v^*)) = \sqrt{\frac{d_{e,res}^2}{3} + u_{C-EO}^2 + u^2(g_e)}, \tag{25c}$$

where the reproducibility variance contribution u_{reprod}^2 is estimated by means of $u(g_e)$, i.e., the standard deviation associated with the prediction interval of the GPR model, which is introduced here to cater to the prediction error including the GPR estimated parameter variability and the residual variability; the traceability contribution u_{trac}^2 is estimated as the combined variance of the calibrated external observer, i.e., the MVS, u_{C-EO}^2 ; the accuracy contribution u_{acc}^2 is estimated considering the average error as half-range variability and assuming a uniform distribution [91]. Here, it is worth remarking that the uncertainty evaluation of the VE, as detailed in Section 3.1, is performed according to LPU-via-VE to estimate the uncertainty of the reproducibility as a prediction interval of the model. Then, further metrological characteristics are added to cater to the accuracy and the presence of the exteroceptive sensor traceability. Future work will investigate the application of other approaches, e.g., PoD-via-VE, to include the uncertainty of the VE embedded in the DT. Expanded uncertainty is evaluated with a coverage factor $k = 2$, resulting in $U(d_{as-is}(d^*, v^*)) = 2.384$ mm, dominated by the systematic error, and in $U(d_{corr}(d^*, v^*)) = 0.254$ mm, thus showing a reduction in uncertainty, thanks to the systematic error correction and the real-time monitoring by means of the MVS, of one order of magnitude, compliant with the target typical error range.

5. Conclusions

Modeling physical systems and characteristics in a virtual environment is key for realizing European strategic policies on sustainability and digitalization. This trend is also reflected by the increasing number of publications on DTs and related topics. However, in order to trust the outcomes of VEs and DTs, traceability and methods for uncertainty evaluation need to be provided.

In this paper, we formally defined VEs and DTs in such a way that the following are fulfilled:

1. The two definitions clearly distinguish between static VEs and time-varying DTs;
2. The definitions are harmonized, allowing for using an VE as a core part (digital model) within a DT, for example, by means of a common mathematical framework; and
3. The definitions allow for considering uncertainties constituting a basis for trustworthy and traceable VEs and DTs.

Furthermore, our definition of a DT is compliant with ISO 23247:2021 and ISO 30173:2023, while better clarifying the DT scope of control of the physical entity by means of the closed-loop feedback control. Our definition of a VE, on the other hand, poses a clear distinction from the terms digital shadow (allowing for automatic updates of the digital model in case that the physical entity changes) and DT (where a change made to the physical entity automatically leads to a change in the digital model and vice versa).

This paper also showed how commonly used uncertainty evaluation methods can be applied in the context of VEs, illustrated by means of the two example methods, LPU and PoD. For DTs, not only the uncertainty of the simulation model (i.e., the virtual part of the DT) needs to be considered, but also the errors and uncertainties related to the sensors (that measure the current state of the system) and the ones related to the actuators (that

control the system). This paper discusses how these contributions can be combined to derive traceability for DTs.

How the uncertainty evaluation methods can be used in industrial applications is shown by means of two test cases, a CMM (as an example for a VE) and a cobot (as an example for a DT). This paper demonstrates the applicability of the metrological framework. Employing a VE in the context of a CMM allows for the calculation of task-specific uncertainties, which is much harder if only the methods of the GUM are being used. By employing a common framework, the way uncertainties are calculated is universal and comprehensible to people not directly involved in the application. The usage of the framework also fosters comparability of measurement results. The DT application allowed the real-time control of the cobot by means of MVS while improving by one order of magnitude the positioning accuracy (from 2.384 mm to 0.254 mm of expanded uncertainty).

For more complex applications, this framework can be adapted and further extended. Within the ViDiT project, this will be done for the following applications: tilted-wave interferometer, virtual flow meter, nanoindentation, highly accurate cylindricity measurement, optical measurements integrated on robot arms, and electrical measurements (see ref. [54]).

Author Contributions: Conceptualization, G.M., M.M., and S.S.; methodology, G.K., G.M., M.M., and S.S.; software, M.v.D., and G.M.; validation, B.A.C., G.G., G.K., and P.P.; formal analysis, M.v.D., G.K., and G.M.; investigation, M.v.D. and G.M.; resources, M.G., and G.K.; data curation, M.v.D., and G.M.; writing—original draft preparation, G.K., G.M., M.M., and S.S.; writing—review and editing, B.A.C., M.v.D., J.F., G.G., M.G., and P.P.; visualization, G.K., and G.M.; supervision, M.G., and S.S.; project administration, S.S.; funding acquisition, S.S., M.G., G.K., P.P., and B.A.C. All authors have read and agreed to the published version of the manuscript.

Funding: This work was carried out within the project 22DIT01 ViDiT, which received funding from the European Partnership on Metrology, cofinanced by the European Union’s Horizon Europe Research and Innovation Programme and by the Participating States.

Data Availability Statement: Dataset available on request from the authors.

Conflicts of Interest: The authors declare no conflicts of interest.

References

1. Jones, D.; Snider, C.; Nassehi, A.; Yon, J.; Hicks, B. Characterising the Digital Twin: A systematic literature review. *CIRP J. Manuf. Sci. Technol.* **2020**, *29*, 36–52. [\[CrossRef\]](#)
2. Flegr, S.; Kuhn, J.; Scheiter, K. When the whole is greater than the sum of its parts: Combining real and virtual experiments in science education. *Comput. Educ.* **2023**, *197*, 104745. [\[CrossRef\]](#)
3. Chinesta, F.; Cueto, E.; Abisset-Chavanne, E.; Duval, J.L.; Khaldi, F.E. Virtual, Digital and Hybrid Twins: A New Paradigm in Data-Based Engineering and Engineered Data. *Arch. Comput. Methods Eng.* **2020**, *27*, 105–134. [\[CrossRef\]](#)
4. Kennedy, M.C.; O’Hagan, A. Bayesian Calibration of Computer Models. *J. R. Stat. Soc. Ser. B Stat. Methodol.* **2001**, *63*, 425–464. [\[CrossRef\]](#)
5. Bayarri, M.; Berger, J.; Cafeo, J.; Garcia-Donato, G.; Liu, F.; Palomo, J.; Parthasarathy, R.; Paulo, R.; Sacks, J.; Walsh, D. Computer model validation with functional output. *Ann. Stat.* **2007**, *35*, 1874–1906. [\[CrossRef\]](#)
6. Fuller, A.; Fan, Z.; Day, C.; Barlow, C. Digital Twin: Enabling Technologies, Challenges and Open Research. *IEEE Access* **2020**, *8*, 108952–108971. [\[CrossRef\]](#)
7. Wright, L.; Davidson, S. How to tell the difference between a model and a digital twin. *Adv. Model. Simul. Eng. Sci* **2020**, *7*, 13. [\[CrossRef\]](#)
8. Wübbeler, G.; Marschall, M.; Kniel, K.; Heißelmann, D.; Härtig, F.; Elster, C. GUM-Compliant Uncertainty Evaluation Using Virtual Experiments. *Metrology* **2022**, *2*, 114–127. [\[CrossRef\]](#)
9. Hughes, F.; Marschall, M.; Wübbeler, G.; Kok, G.; van Dijk, M.; Elster, C. JCGM 101-compliant uncertainty evaluation using virtual experiments. *arXiv* **2024**, arXiv:2404.10530.
10. Scholz, G.; Fortmeier, I.; Marschall, M.; Stavridis, M.; Schulz, M.; Elster, C. Experimental Design for Virtual Experiments in Tilted-Wave Interferometry. *Metrology* **2022**, *2*, 84–97. [\[CrossRef\]](#)
11. Jing, X.; Wang, C.; Pu, G.; Xu, B.; Zhu, S.; Dong, S. Evaluation of measurement uncertainties of virtual instruments. *Int. J. Adv. Manuf. Technol.* **2005**, *27*, 1202–1210. [\[CrossRef\]](#)
12. Kok, G.; Wübbeler, G.; Elster, C. Impact of Imperfect Artefacts and the Modus Operandi on Uncertainty Quantification Using Virtual Instruments. *Metrology* **2022**, *2*, 311–319. [\[CrossRef\]](#)

13. Heißelmann, D.; Franke, M.; Rost, K.; Wendt, K.; Kistner, T.; Schwehn, C. Determination of measurement uncertainty by Monte Carlo simulation. In *Advanced Mathematical and Computational Tools in Metrology and Testing XI*; World Scientific: Singapore, 2018; pp. 192–202. [[CrossRef](#)]
14. Straka, M.; Weissenbrunner, A.; Koglin, C.; Höhne, C.; Schmelter, S. Simulation Uncertainty for a Virtual Ultrasonic Flow Meter. *Metrology* **2022**, *2*, 335–359. [[CrossRef](#)]
15. Weissenbrunner, A.; Ekot, A.K.; Straka, M.; Schmelter, S. A virtual flow meter downstream of various elbow configurations. *Metrologia* **2023**, *60*, 054002. [[CrossRef](#)]
16. Grieves, M. Digital twin: Manufacturing excellence through virtual factory replication. *White Pap.* **2014**, *1*, 1–7.
17. Grieves, M.; Vickers, J. Digital Twin: Mitigating Unpredictable, Undesirable Emergent Behavior in Complex Systems. In *Transdisciplinary Perspectives on Complex Systems: New Findings and Approaches*; Kahlen, F.J., Flumerfelt, S., Alves, A., Eds.; Springer International Publishing: Cham, Switzerland, 2017; pp. 85–113. [[CrossRef](#)]
18. Errandonea, I.; Beltrán, S.; Arrizabalaga, S. Digital Twin for maintenance: A literature review. *Comput. Ind.* **2020**, *123*, 103316. [[CrossRef](#)]
19. Yoon, S.; Koo, J. In situ model fusion for building digital twinning. *Build. Environ.* **2023**, *243*, 110652. [[CrossRef](#)]
20. Zhang, C.; Sun, Q.; Sun, W.; Shi, Z.; Mu, X. Performance-oriented digital twin assembly of high-end equipment: A review. *Int. J. Adv. Manuf. Technol.* **2023**, *126*, 4723–4748. [[CrossRef](#)]
21. Liu, L.; Zhang, X.; Wan, X.; Zhou, S.; Gao, Z. Digital twin-driven surface roughness prediction and process parameter adaptive optimization. *Adv. Eng. Inform.* **2022**, *51*, 101470. [[CrossRef](#)]
22. Cimino, C.; Negri, E.; Fumagalli, L. Review of digital twin applications in manufacturing. *Comput. Ind.* **2019**, *113*, 103130. [[CrossRef](#)]
23. Pang, J.; Zheng, P.; Li, S.; Liu, S. A verification-oriented and part-focused assembly monitoring system based on multi-layered digital twin. *J. Manuf. Syst.* **2023**, *68*, 477–492. [[CrossRef](#)]
24. Verna, E.; Puttero, S.; Genta, G.; Galetto, M. Toward a concept of digital twin for monitoring assembly and disassembly processes. *Qual. Eng.* **2024**, *36*, 453–470. [[CrossRef](#)]
25. Magnanini, M.C.; Tolio, T.A. A model-based Digital Twin to support responsive manufacturing systems. *CIRP Ann.* **2021**, *70*, 353–356. [[CrossRef](#)]
26. Mengke Sun, Z.C.; Zhao, N. Design of intelligent manufacturing system based on digital twin for smart shop floors. *Int. J. Comput. Integr. Manuf.* **2023**, *36*, 542–566. [[CrossRef](#)]
27. Kononowicz, A.A.; Woodham, L.A.; Edelbring, S.; Stathakarou, N.; Davies, D.; Saxena, N.; Car, L.T.; Carlstedt-Duke, J.; Car, J.; Zary, N. Virtual Patient Simulations in Health Professions Education: Systematic Review and Meta-Analysis by the Digital Health Education Collaboration. *J. Med. Internet Res.* **2019**, *21*, e14676. [[CrossRef](#)] [[PubMed](#)]
28. Cellina, M.; Cè, M.; Ali, M.; Irmici, G.; Ibba, S.; Caloro, E.; Fazzini, D.; Oliva, G.; Papa, S. Digital Twins: The New Frontier for Personalized Medicine? *Appl. Sci.* **2023**, *13*, 7940. [[CrossRef](#)]
29. Kasper, L.; Birkelbach, F.; Schwarzmayr, P.; Steindl, G.; Ramsauer, D.; Hofmann, R. Toward a Practical Digital Twin Platform Tailored to the Requirements of Industrial Energy Systems. *Appl. Sci.* **2022**, *12*, 6981. [[CrossRef](#)]
30. Fathy, Y.; Jaber, M.; Nadeem, Z. Digital twin-driven decision making and planning for energy consumption. *J. Sens. Actuator Netw.* **2021**, *10*, 37. [[CrossRef](#)]
31. Ghenai, C.; Husein, L.A.; Al Nahlawi, M.; Hamid, A.K.; Bettayeb, M. Recent trends of digital twin technologies in the energy sector: A comprehensive review. *Sustain. Energy Technol. Assess.* **2022**, *54*, 102837. [[CrossRef](#)]
32. Deng, T.; Zhang, K.; Shen, Z.J.M. A systematic review of a digital twin city: A new pattern of urban governance toward smart cities. *J. Manag. Sci. Eng.* **2021**, *6*, 125–134. [[CrossRef](#)]
33. Dani, A.A.H.; Supangkat, S.H.; Lubis, F.F.; Nugraha, I.G.B.B.; Kinanda, R.; Rizkia, I. Development of a Smart City Platform Based on Digital Twin Technology for Monitoring and Supporting Decision-Making. *Sustainability* **2023**, *15*, 14002. [[CrossRef](#)]
34. Boschert, S.; Rosen, R. Digital Twin—The Simulation Aspect. In *Mechatronic Futures: Challenges and Solutions for Mechatronic Systems and Their Designers*; Hehenberger, P., Bradley, D., Eds.; Springer International Publishing: Cham, Switzerland, 2016; pp. 59–74. [[CrossRef](#)]
35. Schleich, B.; Anwer, N.; Mathieu, L.; Wartzack, S. Shaping the digital twin for design and production engineering. *CIRP Ann.* **2017**, *66*, 141–144. [[CrossRef](#)]
36. Liu, M.; Fang, S.; Dong, H.; Xu, C. Review of digital twin about concepts, technologies, and industrial applications. *J. Manuf. Syst.* **2021**, *58*, 346–361. [[CrossRef](#)]
37. VanDerHorn, E.; Mahadevan, S. Digital Twin: Generalization, characterization and implementation. *Decis. Support Syst.* **2021**, *145*, 113524. [[CrossRef](#)]
38. *ISO 23247-1:2021*; Automation Systems and Integration—Digital Twin Framework for Manufacturing. Part 1: Overview and General Principles. International Organization for Standardization: Geneva, Switzerland, 2021.
39. *ISO/IEC 30173:2023*; Digital Twin—Concepts and Terminology. International Organization for Standardization and International Electrotechnical Commission: Geneva, Switzerland, 2023.
40. Tang, W.; Xu, G.; Zhang, S.; Jin, S.; Wang, R. Digital Twin-Driven Mating Performance Analysis for Precision Spool Valve. *Machines* **2021**, *9*, 157. [[CrossRef](#)]

41. Zhao, Z.; Wang, S.; Wang, Z.; Wang, S.; Ma, C.; Yang, B. Surface roughness stabilization method based on digital twin-driven machining parameters self-adaption adjustment: A case study in five-axis machining. *Int. J. Comput. Integr. Manuf.* **2022**, *33*, 943–952. [[CrossRef](#)]
42. Modoni, G.E.; Stampone, B.; Trotta, G. Application of the Digital Twin for in process monitoring of the micro injection moulding process quality. *Comput. Ind.* **2022**, *135*, 103568. [[CrossRef](#)]
43. Xin, Y.; Chen, Y.; Li, W.; Li, X.; Wu, F. Refined Simulation Method for Computer-Aided Process Planning Based on Digital Twin Technology. *Micromachines* **2022**, *13*, 620. [[CrossRef](#)] [[PubMed](#)]
44. De Ketelaere, B.; Smeets, B.; Verboven, P.; Nicolai, B.; Saeys, W. Digital twins in quality engineering. *Qual. Eng.* **2022**, *34*, 404–408. [[CrossRef](#)]
45. Guo, Y.; Klink, A.; Bartolo, P.; Guo, W.G. Digital twins for electro-physical, chemical, and photonic processes. *CIRP Ann.* **2023**, *72*, 593–619. [[CrossRef](#)]
46. Franciosa, P.; Sokolov, M.; Sinha, S.; Sun, T.; Ceglarek, D. Deep learning enhanced digital twin for Closed-Loop In-Process quality improvement. *CIRP Ann.* **2020**, *69*, 369–372. [[CrossRef](#)]
47. Bergs, T.; Biermann, D.; Erkorkmaz, K.; M'Saoubi, R. Digital twins for cutting processes. *CIRP Ann.* **2023**, *72*, 541–567. [[CrossRef](#)]
48. Karve, P.M.; Guo, Y.; Kapusuzoglu, B.; Mahadevan, S.; Haile, M.A. Digital twin approach for damage-tolerant mission planning under uncertainty. *Eng. Fract. Mech.* **2020**, *225*, 106766. [[CrossRef](#)]
49. Wright, L.; Davidson, S. Digital twins for metrology; metrology for digital twins. *Meas. Sci. Technol.* **2024**, *35*, 051001. [[CrossRef](#)]
50. Zheng, Y.; Wang, S.; Li, Q.; Li, B. Fringe projection profilometry by conducting deep learning from its digital twin. *Opt. Express* **2020**, *28*, 36568–36583. [[CrossRef](#)]
51. Poroskun, I.; Rothleitner, C.; Heißelmann, D. Structure of digital metrological twins as software for uncertainty estimation. *J. Sensors Sens. Syst.* **2022**, *11*, 75–82. [[CrossRef](#)]
52. Härtig, F.; Kniel, K.; Heißelmann, D. Das Virtuelle Koordinatenmessgerät—ein Digitaler Metrologischer Zwilling. *TM-Tech. Mess.* **2023**, *90*, 548–556. [[CrossRef](#)]
53. Shao, G.; Hightower, J.; Schindel, W. Credibility consideration for digital twins in manufacturing. *Manuf. Lett.* **2023**, *35*, 24–28. [[CrossRef](#)]
54. Trustworthy Virtual Experiments and Digital Twins—ViDiT. Available online: <https://www.vidit.ptb.de> (accessed on 13 March 2024).
55. BIPM; IEC; IFCC; ILAC; ISO; IUPAC; IUPAP; OIML. *Evaluation of Measurement Data—Guide to the Expression of Uncertainty in Measurement*; JCGM 100:2008; Joint Committee for Guides in Metrology: Sèvres, France, 2008.
56. BIPM; IEC; IFCC; ILAC; ISO; IUPAC; IUPAP; OIML. *Evaluation of Measurement Data—Supplement 1 to the “Guide to the Expression of Uncertainty in Measurement”—Propagation of Distributions Using a Monte Carlo Method*; JCGM 101:2008; Joint Committee for Guides in Metrology: Sèvres, France, 2008.
57. BIPM; IEC; IFCC; ILAC; ISO; IUPAC; IUPAP; OIML. *Evaluation of Measurement Data—Supplement 2 to the “Guide to the Expression of Uncertainty in Measurement”—Extension to any Number of Output Quantities*; JCGM 102:2011; Joint Committee for Guides in Metrology: Sèvres, France, 2011.
58. Elster, C. Bayesian uncertainty analysis compared with the application of the GUM and its supplements. *Metrologia* **2014**, *51*, S159. [[CrossRef](#)]
59. van Dijk, M.; Kok, G. Comparison of uncertainty evaluation methods for virtual experiments with an application to a virtual CMM. In Proceedings of the IMEKO XXIV World Congress, Hamburg, Germany 26–29 August 2024.
60. Kok, G.; van Dijk, M.; Wübbeler, G.; Elster, C. Virtual experiments for the assessment of data analysis and uncertainty quantification methods in scatterometry. *Metrologia* **2023**, *60*, 044001. [[CrossRef](#)]
61. Marschall, M.; Fortmeier, I.; Stavridis, M.; Hughes, F.; Elster, C. Bayesian uncertainty evaluation applied to the tilted-wave interferometer. *Opt. Express* **2024**, *32*, 18664–18683. [[CrossRef](#)]
62. Possolo, A.; Toman, B. Assessment of measurement uncertainty via observation equations. *Metrologia* **2007**, *44*, 464–475. [[CrossRef](#)]
63. Verna, E.; Genta, G.; Galetto, M.; Franceschini, F. Zero defect manufacturing: A self-adaptive defect prediction model based on assembly complexity. *Int. J. Comput. Integr. Manuf.* **2023**, *36*, 155–168. [[CrossRef](#)]
64. Wu, T.; Yang, F.; Farooq, U.; Li, X.; Jiang, J. An online learning method for constructing self-update digital twin model of power transformer temperature prediction. *Appl. Therm. Eng.* **2024**, *237*, 121728. [[CrossRef](#)]
65. Grieves, M.W. Digital Twins: Past, Present, and Future. In *The Digital Twin*; Crespi, N., Drobot, A.T., Minerva, R., Eds.; Springer International Publishing: Cham, Switzerland, 2023; pp. 97–121. [[CrossRef](#)]
66. Gelman, A.; Carlin, J.B.; Stern, H.S.; Rubin, D.B. *Bayesian Data Analysis*; Chapman and Hall/CRC: New York, NY, USA, 1995.
67. Kyriazis, G.A. Comparison of GUM Supplement 1 and Bayesian analysis using a simple linear calibration model. *Metrologia* **2008**, *45*, L9. [[CrossRef](#)]
68. Balsamo, A.; Di Ciommo, M.; Mugno, R.; Rebaglia, B.; Ricci, E.; Grella, R. Evaluation of CMM uncertainty through Monte Carlo simulations. *CIRP Ann.* **1999**, *48*, 425–428. [[CrossRef](#)]

69. Germer, T.A.; Patrick, H.J.; Silver, R.M.; Bunday, B. Developing an uncertainty analysis for optical scatterometry. In Proceedings of the Metrology, Inspection, and Process Control for Microlithography XXIII, San Jose, CA, USA, 23–26 February 2009; Allgair, J.A., Raymond, C.J., Eds.; International Society for Optics and Photonics: Bellingham, WA, USA, 2009; Volume 7272, p. 72720T. [[CrossRef](#)]
70. van Dorp, B.W.; Haitjema, H.; Delbressine, F.; Bergmans, R.H.; Schellekens, P.H.J. Virtual CMM using Monte Carlo methods based on frequency content of the error signal. In Proceedings of the Recent Developments in Traceable Dimensional Measurements, Munich, Germany, 20–21 June 2001; Decker, J.E., Brown, N., Eds.; International Society for Optics and Photonics: Bellingham, WA, USA, 2001; Volume 4401, pp. 158–167. [[CrossRef](#)]
71. Nath, P.; Mahadevan, S. Probabilistic Digital Twin for Additive Manufacturing Process Design and Control. *J. Mech. Des.* **2022**, *144*, 091704. [[CrossRef](#)]
72. Sisson, W.; Karve, P.; Mahadevan, S. Digital twin for component health- and stress-aware rotorcraft flight control. *Struct. Multidiscip. Optim.* **2022**, *65*, 318. [[CrossRef](#)]
73. Ye, Y.; Yang, Q.; Zhang, J.; Meng, S.; Wang, J. A dynamic data driven reliability prognosis method for structural digital twin and experimental validation. *Reliab. Eng. Syst. Saf.* **2023**, *240*, 109543. [[CrossRef](#)]
74. Thelen, A.; Zhang, X.; Fink, O.; Lu, Y.; Ghosh, S.; Young, B.D.; Todd, M.D.; Mahadevan, S.; Hu, C.; Hu, Z. A comprehensive review of digital twin—Part 2: Roles of uncertainty quantification and optimization, a battery digital twin, and perspectives. *Struct. Multidiscip. Optim.* **2023**, *66*, 1. [[CrossRef](#)]
75. Huang, Z.; Fey, M.; Liu, C.; Beysel, E.; Xu, X.; Brecher, C. Hybrid learning-based digital twin for manufacturing process: Modeling framework and implementation. *Robot.-Comput.-Integr. Manuf.* **2023**, *82*, 102545. [[CrossRef](#)]
76. Carmignato, S.; De Chiffre, L.; Bosse, H.; Leach, R.; Balsamo, A.; Estler, W. Dimensional artefacts to achieve metrological traceability in advanced manufacturing. *CIRP Ann.* **2020**, *69*, 693–716. [[CrossRef](#)]
77. Dahlem, P.; Emonts, D.; Sanders, M.P.; Schmitt, R.H. A Review on Enabling Technologies for Resilient and Traceable on-Machine Measurements. *J. Mach. Eng.* **2020**, *20*, 5–17. [[CrossRef](#)]
78. Jaganmohan, P.; Muralikrishnan, B.; Lee, V.; Ren, W.; Icasio-Hernández, O.; Morse, E. VDI/VDE 2634-1 performance evaluation tests and systematic errors in passive stereo vision systems. *Precis. Eng.* **2023**, *79*, 310–322. [[CrossRef](#)]
79. JCGM 200:2008; International Vocabulary of Metrology—Basic and General Concepts and Associated Terms (VIM). Joint Committee for Guides in Metrology—International Organization for Standardization: Geneva, Switzerland, 2008.
80. Haitjema, H. Uncertainty Estimation in Dimensional Metrology. *Int. J. Precis. Technol.* **2011**, *2*, 226. [[CrossRef](#)]
81. Haitjema, H.; van Dorp, B.W.; Morel, M.; Schellekens, P.H.J. Uncertainty estimation by the concept of virtual instruments. In Proceedings of the Recent Developments in Traceable Dimensional Measurements, Munich, Germany, 20–21 June 2001; Decker, J.E., Brown, N., Eds.; International Society for Optics and Photonics: Bellingham, WA, USA, 2001; Volume 4401, pp. 147–157. [[CrossRef](#)]
82. Ramu, P.; Yagüe, J.; Hocken, R.; Miller, J. Development of a parametric model and virtual machine to estimate task specific measurement uncertainty for a five-axis multi-sensor coordinate measuring machine. *Precis. Eng.* **2011**, *35*, 431–439. [[CrossRef](#)]
83. Vlaeyen, M.; Haitjema, H.; Dewulf, W. Digital Twin of an Optical Measurement System. *Sensors* **2021**, *21*, 6638. [[CrossRef](#)] [[PubMed](#)]
84. Iñigo, B.; Colinas-Armijo, N.; López de Lacalle, L.N.; Aguirre, G. Digital twin-based analysis of volumetric error mapping procedures. *Precis. Eng.* **2021**, *72*, 823–836. [[CrossRef](#)]
85. Maculotti, G.; Genta, G.; Galetto, M. An uncertainty-based quality evaluation tool for nanoindentation systems. *Measurement* **2024**, *225*, 113974. [[CrossRef](#)]
86. Maculotti, G.; Genta, G.; Galetto, M. Optimisation of laser welding of deep drawing steel for automotive applications by Machine Learning: A comparison of different techniques. *Qual. Reliab. Eng. Int.* **2024**, *40*, 202–219. [[CrossRef](#)]
87. ISO 12181-2:2011; Geometrical Product Specifications (GPS)—Roundness—Part 2: Specification Operators. International Organization for Standardization: Geneva, Switzerland, 2011.
88. Nafi, A.; Mayer, R. Identification of scale and squareness errors on a CMM using a step gauge measured based on the ASME 89.4.10360.2-2008 standard. In Proceedings of the 38th Annual North American Manufacturing Research Conference, Kingston, ON, Canada, 25–28 May 2010; Volume 38, pp. 325–332.
89. Maculotti, G.; Genta, G.; Aliev, K.; Galetto, M. Metrological integration and automation of surface topography measuring instruments on cobots. In Proceedings of the 17th CIRP Conference on Intelligent Computation in Manufacturing Engineering, Ischia, Italy, 12–14 July 2023.
90. Verna, E.; Puttero, S.; Genta, G.; Galetto, M. A Novel Diagnostic Tool for Human-Centric Quality Monitoring in Human–Robot Collaboration Manufacturing. *J. Manuf. Sci. Eng.* **2023**, *145*, 121009. [[CrossRef](#)]
91. ISO 14253-2:2011; Geometrical Product Specifications (GPS)—Inspection by Measurement of Workpieces and Measuring Equipment Part 2: Guidance for the Estimation of Uncertainty in GPS Measurement, in Calibration of Measuring Equipment and in Product Verification. International Organization for Standardization: Geneva, Switzerland, 2011.

Disclaimer/Publisher’s Note: The statements, opinions and data contained in all publications are solely those of the individual author(s) and contributor(s) and not of MDPI and/or the editor(s). MDPI and/or the editor(s) disclaim responsibility for any injury to people or property resulting from any ideas, methods, instructions or products referred to in the content.